OPERATIONS RESEARCH
Vol. 54, No. 6, November–December 2006, pp. 1151–1171
ISSN 0030-364X | EISSN 1526-5463 | 06 | 5406 | 1151

DOI 10.1287/opre.1060.0307

An Analytical Model for Traffic Delays and the Dynamic User Equilibrium Problem

Georgia Perakis
Sloan School of Management, Massachusetts Institute of Technology, E53-359, Cambridge, Massachusetts 02139,
georgiap@mit.edu

Guillaume Roels
Anderson School of Management, University of California at Los Angeles, Los Angeles, California 90095,
guillaume.roels@anderson.ucla.edu

In urban transportation planning, it has become critical (1) to determine the travel time of a traveler and how it is affected by congestion, and (2) to understand how traffic distributes in a transportation network. In the first part of this paper, we derive an analytical function of travel time, based on the theory of kinematic waves. This travel-time function integrates the traffic dynamics as well as the effects of shocks. Numerical examples demonstrate the quality of the analytical function, in comparison with simulated travel times. In the second part of this paper, we incorporate the travel-time model within a dynamic user equilibrium (DUE) setting. We prove that the travel-time function is continuous and strictly monotone if the flow varies smoothly. We illustrate how the model applies to solve a large network assignment problem through a numerical example.

Subject classifications: transportation: models assignment; mode/route choice.
Area of review: Transportation.
History: Received March 2004; revisions received December 2004, October 2005; accepted October 2005.

1. Introduction

Over the last 20 years, traffic congestion has grown dramatically, resulting in high environmental costs and productivity losses. According to the Texas Transportation Institute (Schrank and Lomax 2003) on traffic congestion in the United States, "the average delay for every person in the 75 urban areas studied climbed from 7 hours in 1982 to 26 hours in 2001. [...] The total congestion 'invoice' for the 75 areas in 2001 came to $69.5 billion, which was the value of 3.5 billion hours of delay" (pp. 3–4). All the proposed solutions (capacity increase, highway efficiency improvement, demand management) rely on an accurate prediction of traffic congestion. To this end, it has become critical: (1) to determine the travel time of a traveler and how it is affected by congestion, and (2) to understand how traffic distributes in a transportation network.

In this paper, we derive an analytical travel-time function that integrates the traffic dynamics and the effects of shocks. Subsequently, we illustrate how this function can be employed to determine the routes that individual travelers take in a transportation network. In particular, we assume that each user in the system minimizes the time length of his or her own trip, depending on congestion, leading to a dynamic user equilibrium (DUE) in the transportation network.

Analysis of traffic flow can be microscopic or macroscopic. Microscopic models focus on the behavior of a single vehicle, reacting to other vehicles' behavior, and generally adopt a simulation approach (e.g., see Herman et al. 1959, Gazis et al. 1961, Mahut 2000). In contrast, macroscopic models rely on the aggregate behavior of vehicles, depending on surrounding aggregate traffic conditions. Most macroscopic models are based on the theory of kinematic waves in transportation, developed by Lighthill and Whitham (1955) and Richards (1956), that models traffic flow as a compressible fluid in a pipeline. The fluid approach represents the limiting behavior of a stochastic process of a large population, and is therefore appropriate to large-scale problems, such as traffic equilibrium problems on long crowded roads. However, because macroscopic models generally assume a uniform, stationary distribution of traffic, they are generally unable to capture local interactions of vehicles, the time-dependent behavior of traffic within a queue (e.g., the "stop-and-go" phenomenon), and therefore ignore the local triggers of congestion such as traffic controls, turn permissions, opposing traffic streams, etc. Nonetheless, despite these limitations, the theory provides good estimates of the delays caused by queues and their dependence upon entrance and exit flows (Hurdle and Son 2000). In this paper, we derive a function of congestion delays from the theory of kinematic waves.

Over the past decade, most developments based on the theory of kinematic waves have focused on modeling flow

propagation rather than deriving an analytical travel-time function. Newell (1993) modeled flow propagation by using curves of the cumulative number of vehicles at the road entrance and at the road exit. Travel times correspond to the horizontal difference between these two curves. Daganzo (1994, 1995a) proposed an efficient way of propagating flow, by splitting the road into cells. (See also Velan 2000 for enhancements of this model.) His model, called the cell transmission model, is not only very efficient for simulating the transportation network, but can also be formulated as a linear optimization problem (Ziliaskopoulos 2000). While the cell transmission model relies on a triangular flow-density curve, other simulation models rely on a quadratic flow-density curve (see Daganzo 1995b, Khoo et al. 2002).

On the other hand, most traffic assignment models rely on an analytical travel-time function. In fact, traffic assignment problems (such as the DUE problem) can be formulated as nonlinear problems and can be solved with standard optimization algorithms. In particular, when the travel-time function is differentiable, gradient algorithms can be used to solve traffic assignment problems (see Patriksson 1994 for a review). In addition, analytical models allow studying the convergence behavior of these traffic assignment algorithms (e.g., see Friesz et al. 1993, Ran and Boyce 1994).

However, it is unclear which analytical travel-time function should be used in these models. The most generic travel-time function depends on the number of cars, the inflow, and the outflow (see Ran and Boyce 1994). Although Daganzo (1995c) claimed that a travel-time function should depend only on the number of cars on the road, Lin and Lo (2000) pointed out a paradoxical situation with such a function. On the other hand, Carey et al. (2003) introduced a generic travel-time function depending on the average flow rate, satisfying first-in-first-out (FIFO) and other desirable properties. Based on the theory of kinematic waves, Perakis (2000) and Kachani and Perakis (2001) proposed polynomial and exponential travel-time functions for situations without congestion. Based on the simplified kinematic wave model proposed by Newell (1993), Kuwahara and Akamatsu (2001) derived an analytical function of the instantaneous travel time to solve the dynamic user equilibrium. However, the travel time they derived does not represent the actual (or experienced) travel time unless traffic conditions remain constant. Finally, the theory of vertical queues suggests that the travel time can be decomposed into a free-flow travel time and a waiting time in a queue (e.g., see Li et al. 2000). However, these travel-time functions typically do not consider other flow dynamics than the queue, and disregard the spillback effects.

In this paper, we propose a methodology for deriving a polynomial travel-time function on a single stretch of road, based on the theory of kinematic waves. This travel-time model only depends on the traffic conditions at the entrance and at the exit of the road and is therefore less memory intensive than the cell transmission model. We extend the work by Perakis (2000) and Kachani and Perakis (2001) by including congestion into a travel-time function. We also complement the work by Kuwahara and Akamatsu (2001) by analyzing the dynamic user equilibrium with experienced instead of instantaneous travel times. Finally, we generalize the queuing models by integrating the flow dynamics and the spillback effects into the travel-time function. The main contributions of our model are the following:

(1) We develop a methodology for determining travel times analytically that applies to both triangular and quadratic flow-density curves.

(2) We introduce a travel-time function that integrates the first-order traffic dynamics, shocks, and queue spillovers.

(3) From our numerical experiments, it appears that the travel-time function is consistent with the results obtained by simulation.

(4) We establish that the travel-time function satisfies properties such as continuity, monotonicity, and FIFO.

(5) We incorporate the travel-time model within a DUE model.

This paper is organized as follows. In §2, we review the theory of kinematic waves. In §3, we propose a general methodology for deriving a travel-time function and illustrate it within two particular models of flow density (quadratic and triangular). In §4, we discuss the properties of the travel-time function that we derived. In §5, we embed our travel-time function within a more general dynamic user equilibrium problem and illustrate our model through a numerical example. Finally, we conclude by outlining directions for further research.

2. Review of the Theory of Kinematic Waves

In this section, we review the hydrodynamic theory of traffic flow, proposed by Lighthill and Whitham (1955) and Richards (1956). From a macroscopic point of view, the flow of traffic on a stretch of a road can be modeled as the flow of a fluid in a pipeline. Accordingly, traffic flow is animated with waves, moving backwards or forwards.

Because of the dynamic nature of traffic, we work on a time-space plane. The fundamental traffic variables to describe traffic conditions on a road are:

- The flow rate, $f(x, t)$, which is the number of vehicles per hour passing location x at time t,
- the rate of density (or concentration), $k(x, t)$, which is the number of vehicles per mile, at location x at time t, and
- the instantaneous velocity, $v(x, t)$, which is the speed of vehicles passing location x at time t.

Assuming a homogeneous road, these quantities are respectively bounded from above by $f^{\max}$, $k^{\max}$, and $v^{\max}$.

Most models assume a one-to-one relationship between the speed and the density, i.e., $v(x, t) = v(k(x, t))$. This relationship has the additional property that when the density is zero, the speed is equal to the free-flow speed $v^{\max}$,

and when the density is equal to the jam density, $k = k^{\max}$, the speed is zero.

Note that the definition of the fundamental traffic variables implies that $f(x,t) = k(x,t)v(x,t)$. Therefore, the flow and the density are related through the so-called *fundamental diagram*:

$$f(x,t) = k(x,t)v(k(x,t)) \quad \forall x,t. \tag{1}$$

Depending on the assumed speed-density relationship $v(k)$, the fundamental diagram can have different shapes. In what follows, we analyze the two most common shapes, namely, the quadratic and the triangular fundamental diagrams.

Greenshields (1935) modeled the vehicle velocity as a linear function of density, i.e., $v(k) = v^{\max}(1 - k/k^{\max})$. Based on this function, the fundamental diagram has a quadratic shape, as in Richards (1956):

$$f(x,t) = k(x,t)v^{\max}(1 - k(x,t)/k^{\max}). \tag{2}$$

Newell (1993) proposed a triangular curve with a left slope of $1/u_0$ and a right slope of $-1/w_0$. The change of slope occurs when $k = k(f^{\max})$, where $k(f^{\max})$ is the density associated with the road capacity,

$$f(x,t) = \begin{cases} k(x,t)/u_0 \\ \quad \text{if } k(x,t) \leqslant k(f^{\max}) = f^{\max}u_0, \\ (k^{\max} - k(x,t))/w_0 \quad \text{otherwise.} \end{cases} \tag{3}$$

In addition to (1), the traffic variables are related through a conservation law, stated as the following partial differential equation:

$$\frac{\partial k(x,t)}{\partial t} + \frac{df(k)}{dk}\frac{\partial k(x,t)}{\partial x} = 0. \tag{4}$$

This conservation law describes the fact that on a single stretch of road, no cars are lost.

In the time-space plane, a level curve of density is the set of points (x,t) such that $k(x,t)$ remains constant. Because the density uniquely determines the flow according to (2) or (3), the flow $f(k)$ and, by consequence $df(k)/dk$, also remain constant along a level curve of density. Therefore, if $k(x,t)$ remains constant, (4) reduces to the equation of a straight line with slope df/dk. In other words, the level curves of density are straight lines, called characteristic lines.

Characteristic lines represent the propagation of traffic density in the time-space plane. Essentially, density propagates as a wave with speed df/dk. The wave speed (i.e., the slope of the characteristic line), df/dk, is positive when the traffic is light ($k \leqslant k(f^{\max})$) and negative when the traffic is heavy ($k \geqslant k(f^{\max})$). Accordingly, macroscopic traffic conditions propagate forwards when traffic is light and backwards against traffic when traffic is heavy. In particular, with a triangular fundamental diagram, the speed of a wave is $1/u_0$ in light traffic and $-1/w_0$ in heavy traffic. With a quadratic diagram, the wave speed is $v^{\max}(1 - 2k(x,t)/k^{\max})$, which is positive when $k(x,t) \leqslant k^{\max}/2$, and negative otherwise.

It might seem surprising at first to have waves moving in the opposite direction of vehicles. In fact, in many dynamical systems, particles do not move in the same direction as waves. Haberman (1977) illustrates this phenomenon by a horizontal rope, attached to a tree at one end, and vertically moved by a person at the other end. Although waves propagate on the rope from the person to the tree, particles of the rope only move up and down. In transportation, a wave moves backwards when cars are decelerating: The position at which a car begins decelerating is in fact upstream of the position at which the preceding car began decelerating.

If two characteristic lines intersect, the density around the point of intersection is discontinuous. The set of points of intersection is called a shock wave and represents a sudden change in traffic conditions. Behind a bottleneck, a shock wave separates a downstream congested region from an upstream uncongested region. The shock wave propagates backwards when the queue is increasing or forwards when the queue is decreasing.

On the other hand, after an increase of capacity (e.g., when a traffic light turns green), there is a discontinuity of traffic between an upstream congested region and a downstream uncongested region. At the location of the first vehicle in the queue, traffic is discontinuous; hence, the lead vehicle is assumed to accelerate instantaneously, from zero to the free-flow speed. From the lead vehicle's location originates a fan of waves of all possible velocities. In the case of a quadratic fundamental diagram, each of the waves in the fan corresponds to a different density. Accordingly, the following vehicles in the queue accelerate gradually as they pass through the fan of waves. In contrast, in the case of a triangular fundamental diagram, all waves in the fan have the same density $k(f^{\max})$ (as their velocity is a supergradient of the fundamental diagram when the flow is at capacity); hence, the following vehicles in the queues are assumed to accelerate instantaneously, from zero to the free-flow speed.

Figure 1 (borrowed from Lighthill and Whitham's 1955 paper) illustrates a traffic-light cycle. The straight lines are the characteristic lines, the bold line is the shock-wave trajectory, and the dashed line represents a single vehicle's trajectory. When the light turns red, a queue appears behind the traffic light. The characteristic waves in the upstream uncongested region have positive slope, while those in the downstream congested region (i.e., the queue) have negative slope. The two regions are separated by a shock wave that propagates backwards as the queue grows. After the light turns green, the first car in the queue instantaneously accelerates from rest to the free-flow speed. At this point of discontinuity, characteristic lines of all intermediate slopes

Figure 1. A traffic-light cycle.

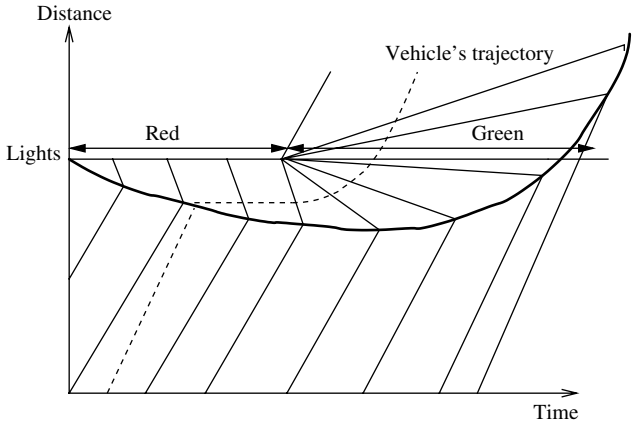

Note. Reprinted with permission of the Royal Society (Lighthill and Whitham 1955, p. 339).

fan out. As the queue clears up, the shock wave moves forwards and passes through the intersection after some time. Note that the represented vehicle crosses various waves during its trip. In particular, in the case of a quadratic fundamental diagram, all waves in the fan have different densities, and the vehicle can increase its speed only slowly, after the light turns green, as it traverses the fan of waves. More details and examples of the theory can be found in Haberman (1977).

3. An Analytical Derivation of the Travel-Time Function

In this section, we propose a general methodology for evaluating the travel time $\tau(L, t_0)$ of a vehicle entering a homogeneous road of length L at time t_0, based on the theory of kinematic waves. In particular, our methodology applies to the triangular and quadratic flow-density curves.

3.1. General Framework

Because of the discontinuity in density induced by shocks, the kinematic wave model may be quite hard to solve. In what follows, we introduce three assumptions that simplify the model.

3.1.1. Assumptions.

ASSUMPTION A1—LINEAR DENSITY. *We assume that the second-order variation of density is locally negligible. Accordingly, for every period t, the density at location x can be approximated by*

$$k(x, t) = k(\xi, t) + B(\xi, t)(x - \xi), \tag{5}$$

where $\xi = 0$ if the traffic conditions at (x, t) are light, and $\xi = L$ if they are heavy. We denote by $B(\xi, t)$ the rate of evolution of the density at time t at the road entrance (if $\xi = 0$) or at the road exit (if $\xi = L$).

We focus on the rate of evolution of the density, instead of the flow, as it might seem more natural, because the value of density carries more information than the value of flow. In particular, from the fundamental diagram, a given flow can be associated with a low or high density, whereas a given density uniquely determines the flow.

Under this assumption, an analytical model of travel time of a vehicle departing at time t_0 and (approximately) arriving at time $t_0 + \theta \geqslant t_0$ (e.g., θ might be chosen to be the free-flow travel time) can be based on the knowledge of only two quantities, $B(0, t_0)$ and $B(L, t_0 + \theta)$. In contrast, an exact model would consider all different values of density $k(x, t)$ of the waves that a vehicle would cross during its trip. If the incoming flow or the exit capacity varies in a very nonlinear fashion, Assumption A1 will be violated. On the other hand, when the flow evolves smoothly, the densities of the waves that the vehicle crosses will not be very different from each other, and the second-order variations will be negligible. In the context of traffic equilibrium, one expects that if the travel demand changes smoothly, the flow on each arc will also evolve smoothly if the path travel-time function is continuous. This intuition has also been confirmed in our numerical example in §5.

In addition, by considering smaller road lengths, a vehicle will cross fewer waves, and hence will encounter less-variable traffic conditions. At the limit, one can consider road segments as small as the cells of Daganzo (1994), on which the flow remains constant. However, improved accuracy would come at the price of greater memory requirements.

In practice, parameters $B(0, t)$ and $B(L, t + \theta)$ will have to be estimated from the traffic conditions at the road entrance and exit, respectively. We suggest estimating $B(0, t + \gamma(t))$ by $(k(0, t) - k(0, t + \gamma(t)))/L$, where $\gamma(t)$ is the time for a forward wave crossing the road entrance at time t to reach the road exit, if there was no shock. In particular, $\gamma(t) = Lu_0$ in the case of a triangular flow-density curve and $\gamma(t) = L/(v^{\max}(1 - 2k(0, t)/k^{\max}))$ in the case of a quadratic flow-density curve. Parameter $B(L, t + \theta)$ can be estimated in a similar way.

The linear relationship of density (5) is not required to be time consistent. That is, assuming a particular value for $k(x, t_0)$ at time t_0 does not imply that there was an actual wave with this density that crossed the road entrance some time before. Instead, Assumption A1 must be considered as a snapshot of the traffic situation from time t_0 onwards, for computing the travel time of a vehicle starting its trip at t_0.

To illustrate the implications of this assumption, let us consider the traffic-light example presented in the last section (Figure 1). Because we consider homogeneous roads, the traffic light must be located at the intersection of two road segments.

Let us first consider the downstream road segment. Suppose that the traffic light has been red for a long time, so that there are only waves of zero density on the road.

Figure 2. When the traffic light turns green—Comparison between the theory of kinematic waves (left) and the simplified model under Assumption A1 (right).

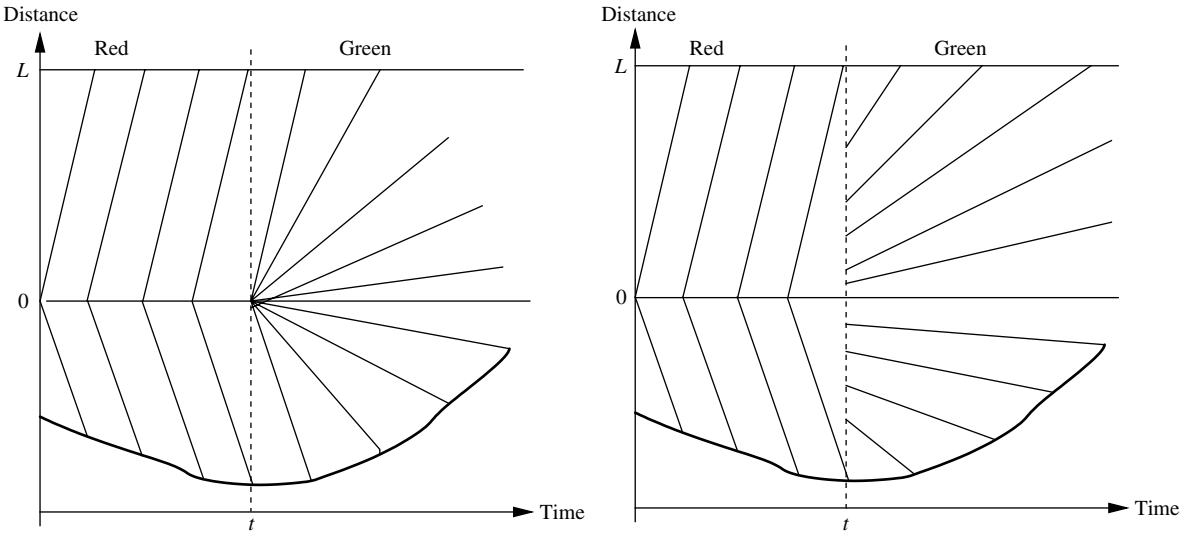

Following the theory of kinematic waves, when the traffic light turns green, the density at the entrance, $k(0,t)$, suddenly jumps to $k(f^{\max})$, while the traffic density at all other points of the road remains zero, i.e., $k(x,t)=0$ for $x \in (0,L]$. From the origin emanates a fan of waves of all possible velocities, as is illustrated in the left part of Figure 2.

Instead, Assumption A1 states that $k(x,t)=k(f^{\max})+B(0,t)x = k(f^{\max})(L-x)/L$, because $B(0,t)=(0-k(f^{\max}))/L$. Therefore, the gradual change of density is still captured under Assumption A1, but the waves associated with these densities do not originate from the same point, as shown in the right part of Figure 2. Similarly, for the upstream segment, Assumption A1 captures the gradual change of density from $k^{\max}$ (at the end of the queue) to $k(f^{\max})$ (at the head of the queue), but the waves do not originate from the same point. Because the waves are more spread out under Assumption A1, the time to exit the queue will be underestimated and the time to accelerate on the downstream road will be overestimated.

Assumption A2—At Most One Shock. *We assume that there is at most one shock on the road, dividing an upstream uncongested region from a downstream congested region.*

In the original model by Lighthill and Whitham (1955) and Richards (1956), a shock may result from the focusing of two forward waves, two backward waves, or one forward and one backward wave. However, as argued by Newell (1993), only the latter type of shocks is observed in reality.

Accordingly, the road can be divided into two segments, separated by the shock wave: On the first segment, the traffic flow has a low density, whereas on the second, it has a high density. If there is no shock, the second segment has zero length, while if heavy-traffic conditions back up to the road entrance, the first segment has zero length.

When the fundamental diagram is triangular, waves in a certain regime all have the same speed; hence, Newell's assumption is automatically satisfied. When the fundamental diagram is quadratic, the assumption holds if $0 \leqslant k(0,t)+B(0,t)L \leqslant k(f^{\max})$ if the traffic conditions at (x,t) are light, and $k(f^{\max}) \leqslant k(L,t)-B(L,t)L \leqslant k^{\max}$ if they are heavy (see the appendix).

Assumption A3—Bounded Variations of Density. *In addition, we require the variations of density to be bounded. Mathematically, we impose the following condition*:

$$|B(\xi,t)| < (k^{\max}-k(\xi,t))^2/(4Lk^{\max}) \quad \text{for } \xi=0 \text{ or } L. \quad (6)$$

This assumption allows us to neglect high-order terms in the travel-time function, as we will show in the proofs of Theorems 1 and 2. If the evolution of traffic flow is highly variable, we can relax (6) by considering smaller road lengths.

3.1.2. Methodology. From Assumption A2, the road can be decomposed into two segments, separated by the shock wave. Therefore, before a vehicle reaches the shock wave, its travel time depends only on the light-traffic conditions, while after the shock wave, its travel time depends only on the heavy-traffic conditions. As a result, as in Ran et al. (1997), the total travel time can be decomposed as the sum of

- the travel time to go from the entrance to the shock wave (under light-traffic conditions), and
- the travel time to go from the shock wave to the road exit (under heavy-traffic conditions).

In particular, let us consider a vehicle that starts its trip at time t_0, on a road of length L. We denote by $\tau(x,t_0)$ its travel time to reach location x. We assume that we know the

traffic conditions (cumulative number of vehicles, density, rate of evolution of density) at the entrance at time t_0 and at the exit at time $t_0+\theta$ for some $\theta \geqslant 0$.

Shock location. A shock is a discontinuity in the traffic flow. Rather than working with flows, Newell (1993) introduced the concept of a cumulative number of vehicles passing through location x by time t, $F(x,t)$. The partial derivatives of $F(x,t)$ correspond to the density and the flow rates, i.e., $\partial F(x,t)/\partial x = -k(x,t)$ and $\partial F(x,t)/\partial t = f(x,t)$.

Along a characteristic line passing through (x_0,t_0) with slope df/dk, the rate of evolution of $F(x,t)$ with respect to x is equal to

$$\frac{dF(x,t)}{dx} = -k(x,t) + f(x,t)\left(\frac{df(k)}{dk}\right)^{-1}. \tag{7}$$

Along a characteristic line, variables k, $f(k)$, and $df(k)/dk$ remain constant, implying that dF/dx also remains constant. Therefore, the knowledge of $F(x_0,t_0)$ and $k(x_0,t_0)$ completely determines the cumulative number of vehicles at each point on the characteristic line.

If the characteristic line has positive slope, $k(x_0,t_0)$ is approximated by $k(0,t_0)+B(0,t_0)x_0$, according to (5). Likewise, $F(x_0,t_0) = F(0,t_0) + \int_0^{x_0} k(x,t)\,dx$ is approximated by $F(0,t_0)+k(0,t)x_0+1/2B(0,t_0)x_0^2$. As a result, the cumulative number of cars at (x,t) is a function of the traffic conditions at the entrance, i.e., a function of $k(0,t_0)$, $B(0,t_0)$, and $F(0,t_0)$. In this case, we denote the cumulative number of vehicles passing x by time t by $A(x,t)$ instead of by $F(x,t)$. We use this notation to emphasize the reference to the cumulative number of arrivals on the road.

Similarly, if the characteristic line has negative slope, the cumulative number of vehicles at (x,t) is a function of the traffic conditions at the exit of the road. In this case, we denote the cumulative number of vehicles passing x by time t by $D(x,t)$ instead of by $F(x,t)$, to emphasize the reference to the cumulative number of departures from the road.

If there was no shock, all characteristic lines would never intersect, and the cumulative number of vehicles would be uniquely determined at every point. However, in the presence of shocks, two characteristic lines could potentially intersect at point (x,t). In such a case, the cumulative number of vehicles at (x,t) would have two different values, namely, $A(x,t)$ and $D(x,t)$. Newell (1993) argued that the correct value for the cumulative number of vehicles passing x by time t is the minimum between $A(x,t)$ and $D(x,t)$, and that the intersection, $A(x,t)=D(x,t)$, determines the shock.

Plugging the vehicle's trajectory $(x, t_0+\tau(x,t_0))$ into the shock wave equation, $A(x,t)=D(x,t)$, gives rise to the point $(\hat{x}, t_0+\hat{\tau})$ at which the vehicle goes through the shock, i.e., $\hat{\tau}=\tau(\hat{x},t_0)$.

Travel-time function in light/heavy traffic. Under Assumption A2, the total travel time can be decomposed as the sum of the travel times before and after the shock.

From the fundamental diagram (1), the instantaneous vehicle's velocity at (x,t) is the ratio between the flow and the density. Accordingly, the vehicle's trajectory $(x, t_0+\tau(x,t_0))$ evolves as follows:

$$\frac{d\tau(x,t_0)}{dx} = \frac{1}{u(x,t_0+\tau(x,t_0))} = \frac{k(x,t_0+\tau(x,t_0))}{f(x,t_0+\tau(x,t_0))}. \tag{8}$$

From the flow-density curve ((2) or (3)), $f(x,t_0+\tau(x,t_0))$ can be expressed as a function of $k(x,t_0+\tau(x,t_0))$. Therefore, the right-hand side of (8) depends only on density.

If the traffic conditions are light at (x,t), the instantaneous velocity (8) can be expressed as a function of the traffic conditions at $(0,t_0)$. Along a characteristic line, the density remains constant; hence, $k(x,t_0+\tau(x,t_0)) = k(x_0,t_0)$, where x_0 is the ordinate at t_0 of the characteristic line passing through $(x,t_0+\tau(x,t_0))$.

Using Assumption A1, $k(x_0,t_0)=k(0,t_0)+B(0,t_0)x_0$. Plugging the density function into (8) gives rise to an ordinary differential equation (ODE). This ODE, together with the initial condition $\tau(0,t_0)=0$, can be solved through a power series expansion (see Edwards and Penney 1985). Under Assumption A3, the ratio between two successive terms in the series is bounded from above by 1, and the series converges.

Similarly, if the traffic conditions are heavy at (x,t), the instantaneous velocity at (x,t) can be expressed as a function of the traffic conditions at $(L,t_0+\theta)$ for some $\theta \geqslant 0$. Denoting by x_θ the ordinate at $t_0+\theta$ of the characteristic line passing through (x,t), we have that $k(x, t_0+\tau(x,t_0)) = k(x_\theta, t_0+\theta)$. Under Assumption A1, $k(x_\theta, t_0+\theta) = k(L,\ t_0+\theta) - B(L,\ t_0+\theta)(L-x_\theta)$. Plugging this function of density into (8) gives rise to an ODE, which can be solved with a power series solution. However, because (x,t) is in the heavy-traffic region, the boundary condition is now defined by the shock location, i.e., $\tau(\hat{x},t_0)=\hat{\tau}$, where $(\hat{x},\hat{\tau})$ solves $A(\hat{x},\ t_0+\tau(\hat{x},t_0+\hat{\tau})) = D(\hat{x},\ t_0+\tau(\hat{x},t_0+\hat{\tau}))$.

Flow propagation. A model of travel time is also a model of flow propagation. In effect, the cumulative number of vehicles at the exit at time $t+\tau(L,t)$ is equal to the cumulative number of vehicles at the entrance at time t, i.e., $A(0,t)=D(L,t+\tau(L,t))$.

However, because of time discretization in numerical experiments, $D(L,t)$ is not defined for the periods t that do not correspond to departure times. Therefore, we have assumed that $D(L,t)$ is piecewise linear between two successive departure times, i.e., for $\lceil \tau(L,t-1)\rceil - 1 \leqslant s \leqslant \lfloor \tau(L,t)\rfloor$,

$$D(L,t+s) = \lambda A(0,t) + (1-\lambda)A(0,t-1), \quad \text{where}$$
$$\lambda = \frac{(t+s)-(t-1+\tau(L,t-1))}{(t+\tau(L,t))-(t-1+\tau(L,t-1))}.$$

At time t, the traffic conditions at the exit are known up to time $t-1+\tau(L,t-1)$ because they depend on the flows that entered the road at or prior to time $t-1$. Therefore, in our numerical experiments, we have chosen $\theta=\lfloor\tau(L,t-1)\rfloor-1$.

For a one-link network, the flow at the road exit, $f(L, t+\theta)$, is set equal to the exit bottleneck capacity Q. For a two-link network, the exit capacity at the end of the upstream link (denoted as link 1) is time varying because a queue may spill back from the downstream link (denoted as link 2). If the queue has uniform density, equal to $k_2(L_2, t+\theta)$, only $k_2(L_2,\ t+\theta)L_2$ vehicles can be present on link 2 at time $t+\theta$. Considering the difference between inflows and outflows, at most $D_2(L_2,\ t+\theta+1)-A_2(0, t+\theta)+k_2(L_2,\ t+\theta)L_2$ vehicles are allowed to enter link 2 in period $t+\theta$. As a result, the capacity at the exit of link 1 is the minimum between Q_2 (static capacity of link 2) and $D_2(L_2,\ t+\theta+1)-A_2(0,\ t+\theta)+k_2(L_2,\ t+\theta)L_2$ (dynamic capacity due to queue spillbacks). If link 1 has several downstream links or link 2 has several upstream links, the same reasoning applies, with additional care of the neighbor links. More details of the general case are presented in §5.

According to Assumption A2, the density at the entrance of the road is taken as the low density associated with the incoming flow $f(0,t)$ and the density at the exit of the road is taken as the high density associated with $f(L,t+\theta)$. As mentioned in the discussion of Assumption A1, $B(0,t+\gamma(t))=(k(0,t)-k(0,t+\gamma(t)))/L$, where $\gamma(t)=L/(df(0,t)/dk)$. Similarly, $B(L,t+\gamma(t))=(k(L,t+\gamma(t))-k(L,t))/L$, where $\gamma(t)=-L/(df(L,t)/dk)$.

In what follows, we apply this general methodology to the triangular and the quadratic fundamental diagrams.

3.2. Triangular Fundamental Diagram

3.2.1. Shock Location. We first show that along the vehicle's trajectory, the cumulative number of vehicles based on the prevailing traffic conditions at the entrance, $A(x,t)$, remains constant. Indeed, when traffic is light, the vehicle is moving at the same speed as the wave conveying the entering flow, $\tau(x,t_0)=xu_0$. Therefore,

$$\begin{aligned}
&A(x,t_0+\tau(x,t_0))\\
&\quad=A(0,t_0)+\left.\frac{dA(\xi,t_0)}{d\xi}\right|_{\xi=0}x,\\
&\quad=A(0,t_0)+(-k(0,t_0)+f(0,t_0)u_0)x \quad \text{from (7)},\\
&\quad=A(0,t_0) \quad \text{from (3)}.
\end{aligned}$$

On the other hand, the cumulative number of vehicles depending on the traffic conditions at the exit, $D(x,t)$, varies along the vehicle trajectory. In contrast to the light-traffic region, the vehicle's trajectory crosses several backward waves.

The cumulative number of vehicles in the heavy-traffic region, $D(x,t)$, is expressed as a function of the traffic conditions at $(L,t_0+\theta)$. The ordinate at $t_0+\theta$ of a characteristic line passing through point $(x,t_0+\tau(x,t_0))$ is $x_\theta=x-(\theta-\tau(x,t_0))/w_0$. Because $dD/d\xi$ remains constant along a characteristic line, from (7), the cumulative number of vehicles based on the traffic conditions at the exit varies as follows:

$$D(x,t_0+\tau(x,t_0))=D(x_\theta,t_0+\theta)+\left.\frac{dD(\xi,t_0+\theta)}{d\xi}\right|_{\xi=x_\theta}(x-x_\theta). \tag{9}$$

From Assumption A1, $D(x_\theta,t_0+\theta)=D(L,t_0+\theta)+k(L,t_0+\theta)(L-x_\theta)-1/2B(L,t_0+\theta)(L-x_\theta)^2$. Replacing $dD/d\xi$ in (9) with (7) gives rise to

$$\begin{aligned}
&D(x,t_0+\tau(x,t_0))\\
&\quad=D(L,t_0+\theta)+k(L,t_0+\theta)(L-x_\theta)\\
&\qquad-\tfrac{1}{2}B(L,t_0+\theta)(L-x_\theta)^2\\
&\qquad+(-k(x_\theta,t_0+\theta)-f(x_\theta,t_0+\theta)w_0)(x-x_\theta)\\
&\quad=D(L,t_0+\theta)+k(L,t_0+\theta)(L-x_\theta)\\
&\qquad-\tfrac{1}{2}B(L,t_0+\theta)(L-x_\theta)^2-k^{\max}(x-x_\theta),
\end{aligned}$$

where the last equality comes from the backward wave speed definition, $w_0f(x_\theta,t_0+\theta)=k^{\max}-k(x_\theta,t_0+\theta)$.

At the shock location, $x_\theta=\hat{x}(1+u_0/w_0)-\theta/w_0$, and the cumulative number of vehicles becomes

$$\begin{aligned}
&D(\hat{x},t_0+\tau(\hat{x},t_0))\\
&\quad=D(L,t_0+\theta)+k(L,t_0+\theta)\left(L+\frac{\theta}{w_0}\right)\\
&\qquad-\tfrac{1}{2}B(L,t_0+\theta)\left(L+\frac{\theta}{w_0}\right)^2\\
&\qquad-k^{\max}\frac{\theta}{w_0}-k(L,t_0+\theta)\hat{x}\left(1+\frac{u_0}{w_0}\right)\\
&\qquad+B(L,t_0+\theta)\hat{x}\left(1+\frac{u_0}{w_0}\right)\left(L+\frac{\theta}{w_0}\right)\\
&\qquad+k^{\max}\hat{x}\frac{u_0}{w_0}-\tfrac{1}{2}B(L,t_0+\theta)\hat{x}^2\left(1+\frac{u_0}{w_0}\right)^2.
\end{aligned}$$

Equating $D(\hat{x},t_0+\tau(\hat{x},t_0))$ to $A(\hat{x},t_0+\tau(\hat{x},t_0))=A(0,t_0)$ gives rise to a quadratic equation in $\hat{x}$. Considering the lower root gives the shock location when the vehicle will go through it.

In particular, when $B(L,t_0+\theta)=0$, the shock location is simply

$$\begin{aligned}
\hat{x}=&\left(D(L,t_0+\theta)-A(0,t_0)\right.\\
&\left.+k(L,t_0+\theta)\left(L+\frac{\theta}{w_0}\right)-k^{\max}\frac{\theta}{w_0}\right)\\
&\cdot\left(k(L,t_0+\theta)\left(1+\frac{u_0}{w_0}\right)-k^{\max}\frac{u_0}{w_0}\right)^{-1}.
\end{aligned} \tag{10}$$

Special case: $\theta=0$. We consider the special case where the available traffic information at the exit is at time t_0. Our goal is to justify why only $D(L,t_0)-A(0,t_0-1)+k(L,t_0)L$ vehicles are authorized to enter the road when a queue spills back.

By definition, $\hat{x}$ is the shock location on the trajectory of a vehicle that enters the road at time t_0. For this reason, when a queue spills back onto upstream links, the shock location $\hat{x}$ must be equal to zero because the entire road is covered by the queue. Therefore, the incoming flow will be constrained to maintain $\hat{x}\geqslant 0$. If $\theta=0$, the shock location (10) is identified as $\hat{x}=(D(L,t_0)-A(0,t_0)+k(L,t_0)L)/(k(L,t_0)(1+u_0/w_0)-k^{\max}(u_0/w_0))$. The denominator is always positive because, from (3), $k(L,t_0)=k^{\max}-f(L,t_0)w_0$ (high-density value) and $(k^{\max}-f(L,t_0)w_0)-f(L,t_0)u_0\geqslant 0$. Therefore, $\hat{x}\geqslant 0$ if the numerator is positive, that is, $D(L,t_0)-A(0,t_0)+k(L,t_0)L\geqslant 0$.

3.2.2. Travel-Time Function. Because a vehicle's speed is constant in light traffic, the travel time to go to the shock location is equal to $u_0\hat{x}$.

On the other hand, the travel time to go from $\hat{x}$ to the road exit is obtained by plugging $f(x,t_0+\tau(x,t_0))=1/w_0(k^{\max}-k(x,t_0+\tau(x,t_0)))$ into (8).

Because the characteristic line passing through $(x,t_0+\tau(x,t_0))$ intersects the time line $t_0+\theta$ at $x_\theta=x-(\theta-\tau(x,t_0))/w_0$, and the density remains constant along a characteristic line, $k(x,t_0+\tau(x,t_0))=k(x_\theta,t_0+\theta)$. Moreover, from (5), $k(x_\theta,t_0+\theta)=k(L,t_0+\theta)-B(L,t_0+\theta)(L-x_\theta)$. Updating (8) gives rise to

$$\frac{d\tau(x,t_0)}{dx}=\frac{(k(L,t_0+\theta)-B(L,t_0+\theta)(L-x_\theta))w_0}{k^{\max}-(k(L,t_0+\theta)-B(L,t_0+\theta)(L-x_\theta))}. \quad (11)$$

As shown in Theorem 1, solving this differential equation gives rise to a closed-form solution of the travel-time function. The static parameters of the obtained travel time are the positive and negative wave paces, u_0 and w_0, and the road length L. On the other hand, the travel time also depends on the dynamic evolution of traffic, namely, the cumulative number of vehicles at the road entrance and at the road exit, $A(0,t_0)$ and $D(L,t_0+\theta)$; the associated densities, $k(0,t_0)$ and $k(L,t_0+\theta)$; and the rate of evolution of the latter with respect to distance, $B(L,t_0+\theta)$. Note that the travel-time function is independent of the rate of evolution of the density at the entrance, $B(0,t_0)$.

To prove Theorem 1, we need a technical assumption about the value of θ. Specifically, we assume that θ is greater than the free-flow travel time up to the shock location and less than the road travel time with a shock.

THEOREM 1. *Under Assumptions* A1 *and* A3, *if* $u_0\hat{x}+(L-\hat{x})w_0k(L,t_0+\theta)/(k^{\max}-k(L,t_0+\theta))\geqslant\theta\geqslant\hat{x}u_0$, *the triangular diagram* (3) *gives rise to the following travel time for a vehicle entering the road at time* t_0:

$$\tau(L,t_0)=\hat{x}u_0+\big(k(L,t_0+\theta)w_0-B(L,t_0+\theta)\cdot(w_0(L-\hat{x})+\theta-u_0\hat{x})\big)\cdot\big(k^{\max}-k(L,t_0+\theta)+B(L,t_0+\theta)\cdot(L-\hat{x}+(\theta-u_0\hat{x})/w_0)\big)^{-1}(L-\hat{x})+O((L-\hat{x})w_0), \quad (12)$$

where $\hat{x}$ *is defined by* (10).

PROOF. The travel time to go from the road entrance to the shock location is $u_0\hat{x}$. On the other hand, the vehicle's trajectory in the heavy-traffic region is given by differential equation (11). Solving the differential equation, together with the boundary condition $\tau(\hat{x},t_0)=u_0\hat{x}$, and using a power series solution, gives rise to (12).

This power series is guaranteed to converge as long as Assumption A3 holds. Indeed, the ratio of two successive terms is bounded from above by

$$\left|\frac{2B(L,t_0+\theta)k^{\max}(L-\hat{x})}{(k^{\max}-k(L,t_0+\theta)+B(L,t_0+\theta)(L-\hat{x}+(\theta-u_0\hat{x})/w_0))^2}\right|,$$

and the series converges if the ratio is bounded from above by 1.

If $B(L,t_0+\theta)\geqslant 0$, an upper bound on the denominator of the ratio is $(k^{\max}-k(L,t_0+\theta))^2$ because both $L-\hat{x}$ and $\theta-u_0\hat{x}$ are positive, by assumption on θ. Hence, the ratio is bounded from above by 1 if $B(L,t_0+\theta)<(k^{\max}-k(L,t_0+\theta))^2/(2Lk^{\max})$, which holds under Assumption A3.

If $B(L,t_0+\theta)\leqslant 0$, the term $(L-\hat{x}+(\theta-u_0\hat{x})/w_0)$ is bounded from above by $(L-\hat{x})(k^{\max}/(k^{\max}-k(L,t_0+\theta)))$, by assumption on θ. Replacing $B(L,t_0+\theta)$ by its lower bound (6) in the denominator, we obtain that the denominator is bounded from below by $(3/4(k^{\max}-k(L,t_0+\theta)))^2$. Hence, the above ratio is less than 1 if $-B(L,t_0+\theta)<9/16(k^{\max}-k(L,t_0+\theta))^2/(2Lk^{\max})$, which holds under Assumption A3. □

3.2.3. Numerical Comparison. Daganzo (1994) proposed a discrete simulation method of flow propagation called the cell transmission model in the case of a triangular flow-density relation. His algorithm is available through a user-friendly software program called Netcell (Cayford et al. 1997). Netcell builds the curves of the cumulative number of vehicles at the entrance and at the exit of the road. The travel time of a vehicle corresponds to the horizontal difference between the two curves.

Figure 3 displays the analytical travel time (12) and the travel time obtained with Netcell, as a function of the departure time. The entering flow evolves quadratically with time, peaking at 1,600 vehicles/hour after 1/2 hour: $f(0,t)=1{,}600-6{,}400(t/3{,}600-0.5)^2$ vehicles/hour for $t=1,\ldots,3{,}600$ seconds. The flow-density relation is asymmetric triangular, with $u_0=1/40$ hour/mile, $w_0=1/10$ hour/mile, and $k^{\max}=200$ vehicles/mile; hence, the road capacity is $f^{\max}=1{,}600$ vehicles/hour. The road has a length of four miles and has a bottleneck at its end authorizing only 1,400 vehicles/hour to exit the road.

Figure 3. Travel time with an exit bottleneck—Comparison between the travel times obtained with the analytical model (12) and the cell transmission model.

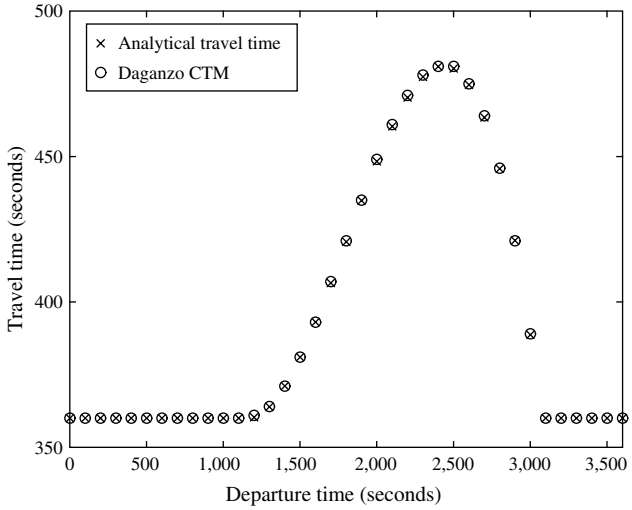

Figure 4. Travel time with queue spillback—Comparison between the travel times obtained with the analytical model (12) and the cell transmission model.

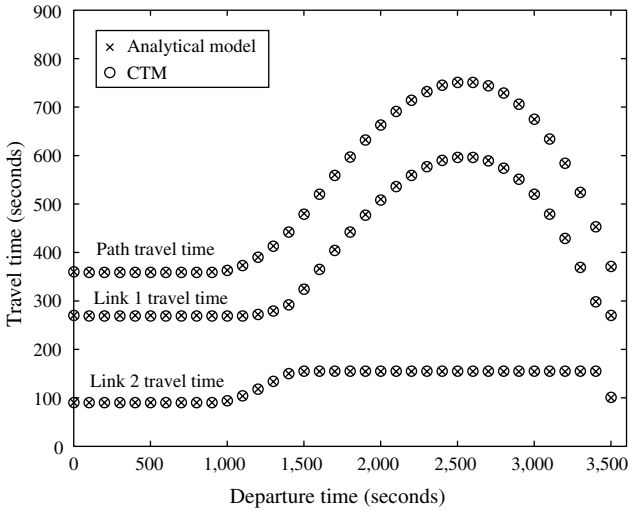

The travel times determine the flow propagation, and the flow propagation determines future travel times (by building the curve $D(L,t)$). In this example, the exit bottleneck capacity is fixed, and $B(L,t)$ is zero for all t.

As illustrated in Figure 3, for each of the 3,600 departure times, the analytical travel-time function practically coincides with the cell transmission model. We performed many different numerical tests (with or without shock, low/high entering flow), and all displayed the same behavior as the example we study in Figure 3.

The next example investigates a queue spillback situation in a two-link network. The lengths of the links are three miles for the first one (upstream) and one mile for the second (downstream). The flow incoming to link 1 is the same as before, but there is now an incoming flow at the entrance of the second link, piecewise linear: $(300-600|t/3{,}600-0.5|)$ vehicles/hour for $t=1,\ldots,3{,}600$. The two links have the same characteristics as above ($u_0=1/40$ hour/mile, $w_0=1/10$ hour/mile, and $k^{\max}=200$ vehicles/mile), and there is a bottleneck at the end of the second link of 1,400 vehicles/hour.

Figure 4 displays the travel time of the downstream link (bottom), the travel time of the upstream link (middle), and the path travel time (top), as a function of the journey departure time, computed with the analytical model (12) and the cell transmission model. As shown in Figure 4, a queue appears behind the bottleneck, at the end of link 2, propagates backwards on link 2, and then spills back into link 1. At this point, the travel time on link 1 starts increasing, while the travel time on link 2 remains constant because the size and the density of the queue remain constant. Note that because the flow incoming to link 2 is time varying, the capacity at the exit of link 1 is also time varying, and $B(L,t+\theta)$ is nonzero. As shown in the figure, both the analytical model and the simulation model give rise to similar travel times.

The final example examines a queue dissipation situation. We consider the same two-link network topology as before, with the same quadratic incoming flow rate. At the end of the first link, after three miles, an incident occurs between periods 1,100 and 1,500, reducing the exit capacity from 1,600 vehicles/hour to 100 vehicles/hour. Figure 5 displays the evolution of the travel times on link 1 (middle), link 2 (bottom), and the total path (top), using the analytical function and the cell transmission model. Note that

Figure 5. Travel time with temporary incidents—Comparison between the travel times obtained with the analytical model (12) and the cell transmission model.

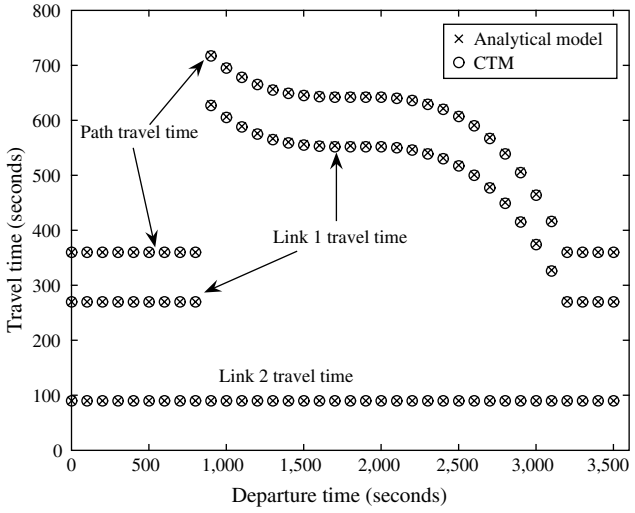

the travel times on link 2 obtained with both methods are equal and correspond to the free-flow travel time, despite the approximation of wave velocities shown in Figure 2. In fact, with a triangular fundamental diagram, all waves that have a pace between u_0 and $-w_0$ have density $k(f^{\max})$ because their slopes correspond to the supergradients of $f^{\max}$ with respect to k; hence, the speed of a vehicle that crosses the fan of waves is $1/u_0$, with or without the linearity assumption. Therefore, Assumption A1 does not affect the travel time in this case.

In summary, in this subsection we analyzed the traffic delays experienced by a traveler on a single stretch of road when the fundamental diagram is triangular. In particular, under Assumptions A1 and A3,

- we proposed a closed-form solution of the shock location;
- we derived a closed-form solution of the travel time, capturing the traffic dynamics and spillback effects, based on the solution of a single ODE; and
- we compared the analytical travel time with Daganzo's cell transmission model, revealing that both models lead to similar results.

3.3. Quadratic Fundamental Diagram

In this section, we derive a travel-time function when the fundamental diagram is quadratic. As we will see, the same methodology applies and the travel-time function that we obtain is also very close to the numerical simulations.

3.3.1. Travel Time Without Shock. From the quadratic fundamental diagram, we substitute $f(x,t_0+\tau(x,t_0))=k(x,t_0+\tau(x,t_0))v^{\max}(1-k(t_0+\tau(x,t_0))/k^{\max})$ into (8).

A characteristic line passing through $(x,t_0+\tau(x,t_0))$ intersects the time origin t_0 at

$$x_0=\frac{x-v^{\max}\tau(x,t_0)(1-2k(0,t_0)/k^{\max})}{1-2v^{\max}\tau(x,t_0)B(0,t_0)/k^{\max}}. \tag{13}$$

Because the density remains constant along a characteristic line, $k(x,t_0+\tau(x,t_0))=k(x_0,t_0)$. Under Assumption A1, $k(x_0,t_0)=k(0,t_0)+B(0,t_0)x_0$. Substituting this linear function of density into (8) gives rise to an ODE. This ODE, together with the initial condition $\tau(0,t_0)=0$, can be solved with a power series solution, giving rise to the following analytical function of travel time in light traffic:

$$\tau(x,t_0)=\frac{x}{v^{\max}(1-k(0,t_0)/k^{\max})}+\frac{1}{2}\frac{B(0,t_0)k(0,t_0)x^2}{(k^{\max})^2v^{\max}(1-k(0,t_0)/k^{\max})^3}+O\left(\frac{L}{v^{\max}}\right). \tag{14}$$

This power series converges under Assumption A3 because the ratio of two successive terms is bounded above by $|2B(0,t)L(k^{\max}/(k^{\max}-k(0,t))^2)|$, which is less than 1 under Assumption A3. Note that if there is no variation in density, i.e., $B(0,t)=0$, the travel time (14) reduces to the ratio of distance over speed.

3.3.2. Shock Location. Unlike with the triangular fundamental diagram, the vehicle's trajectory crosses several waves in light traffic when the fundamental diagram is quadratic. Nonetheless, the cumulative number of vehicles depending on the prevailing conditions at the road entrance, $A(x,t)$, remains constant along the vehicle's trajectory. Let us denote by x_0 the ordinate at t_0 of the characteristic line passing through $(x,t_0+\tau(x,t_0))$. From (7), the cumulative number of vehicles along the vehicle's trajectory is equal to

$$\begin{aligned}&A(x,t_0+\tau(x,t_0))\\&=A(x_0,t_0)+\left.\frac{dA(\xi,t_0)}{d\xi}\right|_{\xi=x_0}(x-x_0)=A(x_0,t_0)\\&\quad+\left(-k(x_0,t_0)+\frac{k(x_0,t_0)(1-k(x_0,t_0)/k^{\max})}{1-2k(x_0,t_0)/k^{\max}}\right)(x-x_0)\\&=A(0,t_0)-\int_0^{x_0}k(x,t_0)\,dx\\&\quad+\left(-k(x_0,t_0)+\frac{k(x_0,t_0)(1-k(x_0,t_0)/k^{\max})}{1-2k(x_0,t_0)/k^{\max}}\right)(x-x_0).\end{aligned}$$

Replacing x_0 by (13), and $\tau(x,t_0)$ by the nth order expansion of (14) into the above expression of $A(x,t_0+\tau(x,t_0))$, and finally taking the nth order Taylor series expansion around $x=0$, we obtain that

$$A(x,t_0+\tau(x,t_0))=A(0,t_0)+O(x^n).$$

Therefore, similarly to the triangular case, the cumulative number of vehicles remains constant along the vehicle's trajectory, despite the fact that the vehicle crosses waves of different densities.

On the other hand, $D(x,t)$ is expressed as a function of the traffic conditions at $(L,t_0+\theta)$. Let x_θ be the ordinate at $t_0+\theta$ of the characteristic line passing through $(x,t_0+\tau(x,t_0))$. To simplify the computations, we assume that the density is constant in the heavy-traffic region. Therefore, the characteristic line has a slope of $v^{\max}(1-2k(L,t_0+\theta)/k^{\max})$ and $x_\theta=x+(\theta-\tau(x,t_0))v^{\max}(1-2k(L,t_0+\theta)/k^{\max})$. From (7),

$$\begin{aligned}&D(x,t_0+\tau(x,t_0))\\&=D(x_\theta,t_0+\theta)+\left.\frac{dD(\xi,t_0+\theta)}{d\xi}\right|_{\xi=x_\theta}(x-x_\theta)\\&=D(L,t_0+\theta)+k(L,t_0+\theta)(L-x_\theta)\\&\quad+\left(-k(L,t_0+\theta)+\frac{f(L,t_0+\theta)}{v^{\max}(1-2k(L,t_0+\theta)/k^{\max})}\right)(x-x_\theta).\end{aligned}$$

At the shock location, the vehicle's travel time $\tau(\hat{x},t_0)$, denoted by $\hat{\tau}$, is defined as in (14), with $\hat{x}$ instead of x. Plugging $\tau(\hat{x},t_0)$ into x_θ defines the cumulative number of vehicles at the shock location as follows:

$$D(\hat{x},t_0+\tau(\hat{x},t_0))=D(L,t_0+\theta)+k(L,t_0+\theta)\cdot(L-\hat{x})\frac{k(L,t_0+\theta)-k(0,t_0)}{k^{\max}-k(0,t_0)}.$$

A shock occurs when $A(\hat{x}, t_0+\tau(\hat{x}, t_0)) = D(\hat{x}, t_0+\tau(\hat{x}, t_0))$, i.e., at location

$$\hat{x} = L - (A(0,t_0) - D(L, t_0+\theta)) \cdot \frac{k^{\max} - k(0,t_0)}{k(L,t_0+\theta)(k(L,t_0+\theta)-k(0,t_0))}. \quad (15)$$

3.3.3. Travel-Time Function with Shocks. In this subsection, we integrate the effects of a shock into the travel-time function. As with the triangular flow-density curve, the resulting travel-time function has a closed form and depends on static road features (maximum speed $v^{\max}$, jam density $k^{\max}$, and length L) and on the dynamic evolution of the cumulative number of vehicles at the entrance and at the exit, $A(0,t_0)$ and $D(L,t_0+\theta)$; the associated densities, $k(0,t_0)$ and $k(L,t_0+\theta)$; and their rate of evolution, $B(0,t_0)$ and $B(L,t_0+\theta)$. Similarly to the triangular case, we need a technical assumption on the value of θ to prove the theorem. Specifically, we assume that it is greater than the free-flow travel time up to the shock and less than the road travel time with the shock.

THEOREM 2. *Under Assumptions* A1–A3, *if* $\hat{\tau} + (L-\hat{x})/(v^{\max}(1-k(L,t_0+\theta)/k^{\max})) \geqslant \theta \geqslant \hat{\tau}$, *the quadratic diagram* (2) *gives rise to the following travel time for a vehicle entering the road at time* t_0:

$$\tau(L,t_0) = \hat{\tau} + \big((k^{\max} + 2v^{\max}(\theta-\hat{\tau})B(L,t_0+\theta))(L-\hat{x})\big) \cdot \big(v^{\max}(k^{\max} - k(L,t_0+\theta) + B(L,t_0+\theta) \cdot (L-\hat{x}+v^{\max}(\theta-\hat{\tau})))\big)^{-1} + O\left(\frac{L-\hat{x}}{v^{\max}}\right), \quad (16)$$

where $\hat{x}$ *is defined in* (15) *and* $\hat{\tau} = \tau(\hat{x}, t_0)$ *according to* (14).

PROOF. We obtain an ODE representing the instantaneous velocity of a vehicle in a similar fashion as in the case of light traffic. However, the boundary condition is defined at the shock location, $\tau(\hat{x}, t_0) = \hat{\tau}$, where $\tau(\hat{x}, t_0)$ is the time to reach the shock, using (14). Using a power series solution to solve the differential equation, together with the boundary condition, gives rise to (16). The ratio between two successive terms in this power series is bounded from above by

$$\left| \frac{2B(L,t_0+\theta)(k^{\max} + 2v^{\max}B(L,t_0+\theta)(\theta-\hat{\tau}))(L-\hat{x})}{(k^{\max} - k(L,t_0+\theta) + B(L,t_0+\theta)(L-\hat{x}+v^{\max}(\theta-\hat{\tau})))^2} \right|,$$

and the series converges if this ratio is less than 1.

If $B(L,t_0+\theta) \geqslant 0$, the denominator of the ratio is bounded from above by $(k^{\max} - k(L,t_0+\theta))^2$ because both $L-\hat{x}$ and $\theta-\hat{\tau}$ are positive, by assumption on θ. Replacing $B(L,t_0+\theta)$ by its upper bound (6) in the numerator, we obtain that the numerator is bounded from above by $2B(L,t_0+\theta)(k^{\max} + 1/2(k^{\max} - k(L,t_0+\theta))) < 5/2B(L,t_0+\theta)k^{\max}$ because $k(L,t_0+\theta) \geqslant k^{\max}/2$. Hence, the ratio is bounded by 1 if $B(L,t_0+\theta) < 2/5(k^{\max} - k(L,t_0+\theta))^2/(Lk^{\max})$, which holds under Assumption A3.

If $B(L,t_0+\theta) \leqslant 0$, the term $(L-\hat{x}+v^{\max}(\theta-\hat{\tau}))$ is bounded from above by $(L-\hat{x})(2k^{\max} - k(L,t_0+\theta))/(k^{\max} - k(L,t_0+\theta))$, by assumption on θ. Replacing $B(L,t_0+\theta)$ by its lower bound (6) in the denominator, we obtain that the denominator is bounded from below by $((k^{\max} - k(L,t_0+\theta))(1 - 1/4(2 - k(L,t_0+\theta)/k^{\max})))^2$. Because $k(L,t_0+\theta) \leqslant k^{\max}$, the denominator is bounded from below by $(3/4(k^{\max} - k(L,t_0+\theta)))^2$. Hence, the ratio is less than 1 if $-B(L,t_0+\theta) < 9/16(k^{\max} - k(L,t_0+\theta))^2/(2Lk^{\max})$, which holds under Assumption A3. □

3.3.4. Numerical Comparison. We compared the analytical travel time (16) with several travel-time functions that were proposed in the literature, all based on the theory of kinematic waves, obtained either via simulation or via an analytical derivation.

In the case of a quadratic fundamental diagram, Kachani and Perakis (2001) derived two functions (polynomial and exponential) of travel time. On the other hand, Khoo et al. (2002) simulated the flow propagation along Godunov's scheme for calculating the numerical flux. They used two different methods, called hyperbolic partial differential equations (PDE) and iterative position update methods. Finally, Daganzo (1995b) approximated the kinematic wave model with finite difference equations (FDE) and simulated flow propagation accordingly. The travel time is the horizontal difference between the cumulative departures and the cumulative arrivals on the road.

In Figure 6, we consider a quadratic incoming flow rate $f(0,t) = 1{,}600 - 6{,}400(t/3{,}600 - 0.5)^2$ vehicles/hour for $t = 1, \ldots, 3{,}600$ seconds. The road has a length of four miles, a maximum speed $v^{\max} = 40$ miles/hour, a maximum density $k^{\max} = 200$ vehicles/mile, and hence, a capacity of $f^{\max} = 2{,}000$ vehicles/hour. There is no exit bottleneck. The $\times$-marks represent the analytical travel time derived in Theorem 2. The three top lines are the travel times obtained by simulation by Khoo et al. (KLPP) and Daganzo (D), and the two bottom lines are the analytical functions proposed by Kachani and Perakis (KP). As illustrated in the figure, the analytical travel-time function (16) is very close to what was obtained from the simulations.

The second example investigates the evolution of travel times in the presence of an exit bottleneck of 1,500 vehicles/hour. In this example, we only compared the analytical travel time (16) with Daganzo's FDE model. In fact, the simulation results obtained by Khoo et al. (2002) were not available to us in this case, and the analytical travel-time functions proposed by Kachani and Perakis (2001) are only valid under light traffic. As illustrated in Figure 7, both the analytical model (16) and the FDE simulation model lead to similar travel times. We obtained comparable results with larger incoming flows.

Because the bottleneck capacity remains constant over time, $B(L,t+\theta) = 0$. On the other hand, the incoming

Figure 6. Travel time under light traffic, with a quadratic incoming flow rate—Comparison among the travel times obtained with the analytical model (16), the analytical models by Kachani and Perakis (2001), the simulations by Khoo et al. (2002), and the finite difference equation simulations by Daganzo (1995b).

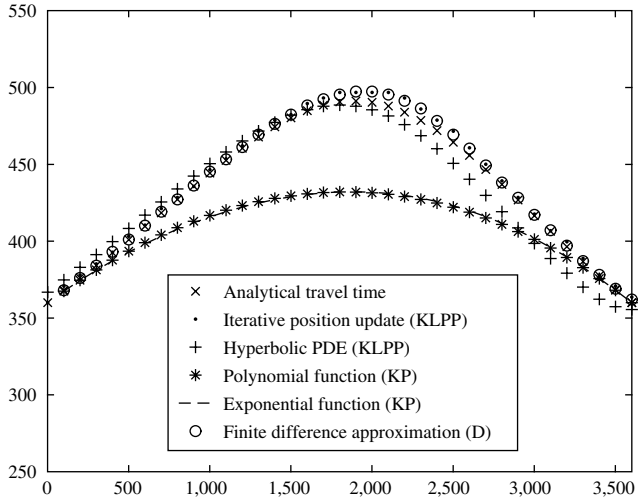

flow is time varying, and $B(0,t)$ is different than zero. In contrast, most models of vertical queues ignore the flow dynamics, setting $B(0,t)$ to zero. As illustrated in Figure 7, although a model of a vertical queue gives a good approximation of the simulated travel time, it is not as accurate as the analytical model (16).

The last example analyzes a situation with a queue dissipation. We consider the same quadratic entering flow and

Figure 7. Travel time with an exit bottleneck—Comparison between the travel times obtained with the analytical model (16) and the finite difference equation simulations by Daganzo (1995b).

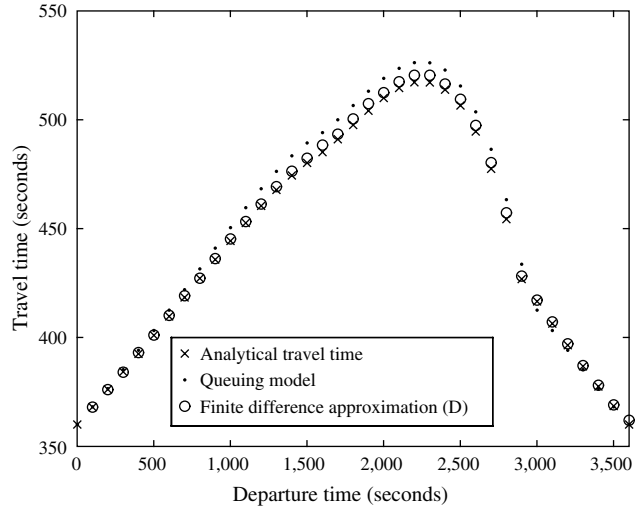

Figure 8. Travel time with an incident—Comparison between the travel times obtained with the analytical model (16) and the finite difference equation simulations by Daganzo (1995b).

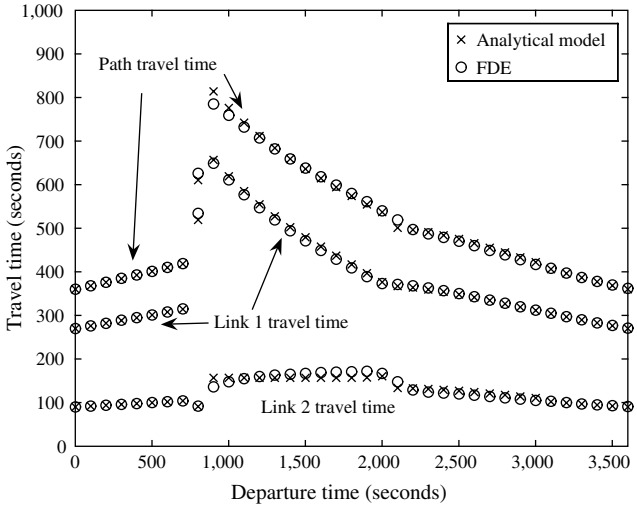

the same road characteristics as before. We assume that an incident occurs at mile 3 after 1,100 seconds, causing a temporary bottleneck of 100 vehicles/hour (in lieu of 2,000 vehicles/hour) until time 1,500. Figure 8 displays the travel times on the first three miles (middle), on the last mile (bottom), and on the total link (top), as a function of the departure time, obtained with the analytical model (16) and the FDE simulation model. The parameter $B(0,t)$ was constrained to be no larger than (6) to ensure convergence of the series expansion of (16). The travel time on the first three miles computed with (16) is slightly larger than the travel time obtained with simulation. In fact, the travel time (16) is evaluated in reference to the exit capacity at time $t+\theta = t-1+\lfloor \tau(t-1) \rfloor$ and identifies the capacity increase at the end of the incident with a one-period lag.

On the other hand, the travel time on the last mile obtained with (16) slightly overestimates the one obtained by simulation, just after the removal of the bottleneck. In fact, Assumption A1 approximates the fan of waves appearing just after the bottleneck removal (see Figure 2). Because low-density waves are located farther from the entrance under Assumption A1, the analytical travel-time function (16) overestimates the simulated travel time on the downstream road segment. On the other hand, after the queue has cleared up, the analytical travel time (16) underestimates the one obtained by simulation. In fact, the analytical travel time, based on Assumption A2, ignores the shock occurring between low-density upstream flow and higher, but still low, density downstream flow.

In summary, in this subsection, we analyzed the traffic delays experienced by a traveler on a single stretch of road, in the case of a quadratic fundamental diagram. In particular, under Assumptions A1, A2, and A3,

- we proposed a closed-form solution of the shock location, assuming constant density in the heavy-traffic region;
- we derived a closed-form solution of the travel time, capturing the traffic dynamics, based on the solution of a single ODE;
- we highlighted the quality of prediction of the analytical travel time in comparison to simulations.

4. Properties of the Travel-Time Function

In this section, we analyze some common properties of the two travel-time functions that we derived in §3. First, we consider two particular cases, namely, when θ corresponds to the free-flow travel time and when $t+\theta$ corresponds to the departure time of the flow that arrived one period earlier. Note that these two particular cases satisfy the conditions of Theorems 1 and 2. Second, we prove that the travel-time function is continuous, monotone, and satisfies the FIFO property under certain conditions.

4.1. Two Particular Cases

4.1.1. θ = Free-Flow Travel Time. When θ corresponds to the free-flow travel time and the dynamic effects are neglected, the travel-time functions (12) and (16) are very intuitive, as shown in the next corollary.

COROLLARY 1. *When θ equals the free-flow travel time (Lu_0 under a triangular fundamental diagram, and $L/(v^{\max}(1-k(0,t)/k^{\max}))$ under a quadratic fundamental diagram), and when $B(0,t)=B(L,t+\theta)=0$, the travel-time functions* (12) *and* (16) *simplify to*

$$\tau(L,t)=\theta+\frac{A(0,t)-D(L,t+\theta)}{f(L,t+\theta)}. \tag{17}$$

Under the assumptions of Corollary 1, the travel-time function can be decomposed as the sum of

- the time to travel a distance L at the free-flow speed, θ, and
- the time to wait in a queue for available downstream capacity,

$$\frac{A(0,t)-D(L,t+\theta)}{f(L,t+\theta)}.$$

Such a travel-time model is very similar to the traditional point queue models (e.g., see Li et al. 2000). However, queuing models usually assume that the exit capacity is fixed, i.e., $f(L,t+\theta)=Q$. In this particular case, despite the fact that $B(0,t)=B(L,t+\theta)=0$, the exit capacity might be different for each period of incoming flow.

4.1.2. $t+\theta$ = Departure Time of the Flow That Arrived in Period $t-1$. When $t+\theta$ corresponds to the departure time of the flow that arrived in period $t-1$, and when $B(0,t)=B(L,t+\theta)=0$, the expression for the travel-time function greatly simplifies and is insightful. Note that when we compute the travel time of the incoming flow at time t, time $t+\theta=t-1+\tau(t-1)$ corresponds to the last period for which we have traffic information at the exit.

COROLLARY 2. *When $\theta=\tau(t-1)-1$ and $B(0,t)=B(L,t+\theta)=0$, the travel-time functions* (12) *and* (16) *simplify to*

$$\tau(L,t)=\tau(L,t-1)-1+\frac{f(0,t)}{f(L,t+\theta)}. \tag{18}$$

The corollary follows from the fact that when $\tau(L,t)=\tau(L,t-1)-1$, $D(L,t+\theta)=A(0,t-1)$, and $f(0,t)=A(0,t)-A(0,t-1)$.

Therefore, the departure time of a flow incoming at time t, i.e., $t+\tau(L,t)$, is the sum of

- the departure time of the flow that arrived one period before, and
- the time to wait for the incoming flow to exit, at the rate defined by the exit capacity at time $t+\theta$.

Although both particular cases assume $B(0,t)=B(L,t+\theta)=0$, the second case is actually more accurate than the first one. Figure 9 illustrates a situation where a vehicle departing at time t is in a queue, assuming a triangular fundamental diagram. The horizontal distance between the curves of the cumulative number of vehicles corresponds to the travel time. The slope of the cumulative number of vehicles at the exit is changing over time because the exit capacity is time varying (e.g., due to the changing traffic on neighbor roads).

The first case considers $\theta=Lu_0$. The travel time is the sum of θ and the size of the queue, $A(0,t)-D(L,t+\theta)$, divided by the exit capacity $f(L,t+Lu_0)$. Because the difference between the experienced travel time and the free-flow travel time can be large, approximating the average capacity between $t+\theta$ and $t+\tau(L,t)$ with $f(L,t+\theta)$ might lead to a poor estimation of the travel time.

The second case considers $\theta=\tau(L,t-1)-1$. The travel time is the sum of θ and the incoming flow $f(0,t)$ divided by the exit capacity $f(L,t-1+\tau(L,t-1))$. Because the difference between the departure times of two successive vehicles, $\tau(L,t)+1-\tau(L,t-1)$, typically covers few periods, the average capacity between $t-1+\tau(L,t-1)$ and $t+\tau(L,t)$ will be fairly accurately approximated with $f(L,t-1+\tau(L,t-1))$ (in the figure, they are equal). As a result,

Figure 9. Evolution of the cumulative number of cars at the entrance and at the exit.

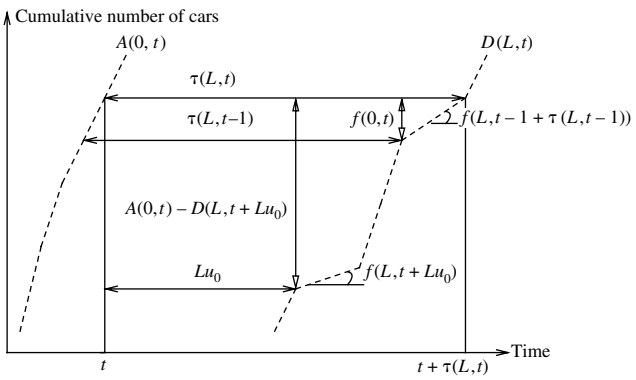

the approximation of the travel time with $\theta=\tau(t-1)-1$ will in general be more accurate than that with θ equal to the free-flow travel time.

In fact, even if $B(L,t+\theta)=0$, the travel-time function (18) integrates the changes of exit capacity that occurred prior to $t-1+\tau(L,t-1)$ because it is defined recursively. The rate of change of the exit capacity $B(L,t+\theta)$ only matters for describing changes in traffic conditions between $t-1+\tau(L,t-1)$ and $t+\tau(L,t)$, which typically covers few periods.

In the example of Figure 4, $B(L,t+\theta)$ was assumed to be nonzero to capture the dynamics of the entering traffic onto link 2. However, considering a nonzero value of $B(L,t+\theta)$ led to some numerical instability if the travel time (12) was truncated to low orders. In particular, truncating the travel-time function to low orders gives rise to a chain of errors: Inaccurate travel times lead to inaccurate flow propagation, and vice versa. To ensure numerical stability, we had to consider a 15th order series expansion of the travel time (12). In contrast, taking $B(L,t+\theta)$ equal to zero is very stable numerically. Moreover, the travel times computed with (18) are still very accurate: In the example of Figure 4, the maximum relative difference between the 15th order series expansion of (12) and (18) was 0.25%.

This observation also holds in a less restrictive environment, when $B(0,t)$ is not required to be zero (under a quadratic diagram).

4.2. Continuity and Monotonicity

Continuity and strict monotonicity of the travel-time function are desirable properties for solving the dynamic traffic equilibrium problem. In particular, the DUE problem can be formulated as a variational inequality over a compact set (see Nagurney 1993). If the travel-time function is continuous, the variational inequality has a solution. If the travel-time function is strictly monotone, the variational inequality has at most one solution.

In what follows, we assume that θ is smaller than or equal to $\tau(L,t-1)-1$ and is independent of the incoming flow. Accordingly, the traffic quantities at the road exit (i.e., $D(L,t+\theta), f(L,t+\theta)$) are independent of the entering flow. For instance, the conditions are met if $\theta=\tau(L,t-1)-1$ or if θ corresponds to the free-flow travel time under a triangular fundamental diagram. However, with a quadratic fundamental diagram, when θ corresponds to the free-flow travel time, it depends on the incoming flow, as $\theta=L/(v^{\max}(1-k(0,t)/k^{\max}))$.

THEOREM 3. *If $\theta\leqslant\tau(L,t-1)-1$ and is independent of the incoming flow, the travel-time functions* (12) *and* (16) *are continuous.*

PROOF. The shock locations (10) and (15) are continuous functions of $A(0,t_0)$. Because both travel-time functions in light traffic (xu_0 and (14)) are continuous functions of x and $k(0,t)$, and the travel-time functions (12) and (16) are continuous functions of $\hat{\tau}$, it follows that the travel-time functions are continuous. □

THEOREM 4. *If $\theta\leqslant\tau(L,t-1)-1$ and is independent of the incoming flow, there exists a range of values for $B(0,t)$ and $B(L,t+\theta)$ around zero, for which the travel-time functions* (12) *and* (16) *are monotone and strictly monotone functions of flow, respectively.*

PROOF. Proving the (strict) monotonicity of a function is equivalent to showing that its Jacobian matrix is positive semidefinite (positive definite) (see Nagurney 1993). The (i,j)th entry of the Jacobian is the derivative of the travel time of the ith period with respect to the flow incoming in the jth period. In what follows, we consider the derivatives of the travel times with the incoming densities, as there is a one-to-one relation between the incoming flow and the incoming density (recall that from Assumption A2, we always have $k(0,t)\leqslant k(f^{\max})$).

In the remainder of the proof, we show that if $B(0,t)$ and $B(L,t+\theta)$ are in some intervals around zero, the Jacobian matrix is lower triangular, with nonnegative diagonal entries. In particular, if the fundamental diagram is quadratic, all diagonal entries are positive, and the Jacobian is positive definite. If the fundamental diagram is triangular, some diagonal entries might be equal to zero, and the Jacobian matrix is positive semidefinite.

Let us first consider the case without shocks. The free-flow travel time consistent with a triangular fundamental diagram is independent of flow. As a result, if there is no shock in period i, the entire ith row in the matrix is zero. On the other hand, with a quadratic fundamental diagram, the travel time under light traffic depends on the entering flow, both through $k(0,t)$ and $B(0,t)$. In the following, we assume that $B(0,t+\gamma(t))=(k(0,t)-k(0,t+\gamma(t)))/L$, with $\gamma(t)=L/(df(0,t)/dk)\geqslant 0$. (Simpler results can be derived if $B(0,t)$ is independent of the incoming flow.) The travel time in period $t+\gamma(t)$ is a function of $k(0,t)$ and $k(0,t+\gamma(t))$; hence, the travel time depends only on past flows. Considering the first-order travel-time function (14), the diagonal elements of the Jaobian matrix are of the form

$$\frac{d\tau(L,t)}{dk(0,t)}=\frac{L(k^{\max}-(3/2)k(0,t))k^{\max}}{v^{\max}(k^{\max}-k(0,t))^3}+\frac{B(0,t)L^2(k^{\max}+2k(0,t))k^{\max}}{2v^{\max}(k^{\max}-k(0,t))^4}.$$

Therefore, if $B(0,t)$ is in some interval $[-\underline{B}_{\text{low}},\infty)$ around zero, $d\tau(L,t)/dk(0,t)>0$. The travel times in periods other than t and $t+L/(df(0,t)/dk)$ are independent of $k(0,t)$; hence, their derivative with respect to $k(0,t)$ is zero.

Let us now introduce shocks into the travel-time functions. Independently of the shape of the fundamental diagram, the shock location for a vehicle departing at time t, (10) and (15), decreases linearly with the flows that have started in periods $s\leqslant t$ and that have not left the road at $t+\theta$, i.e., $s+\tau(L,s)<t+\theta$, through $A(0,t)-D(L,t+\theta)$.

In addition, one can show that the travel time with shocks is a decreasing function of the shock location if $B(L,t+\theta)$

is in some interval $[-\underline{B}_{\text{high}}, \bar{B}_{\text{high}}]$ around zero. In the case of a triangular fundamental diagram, the derivative of the first-order travel-time function (12) with respect to the shock location,

$$\frac{d\tau(L,t)}{d\hat{x}} = u_0 + w_0 - k^{\max}\frac{w_0(k^{\max}-k(L,t+\theta))+B(L,t+\theta)(\theta-u_0 L)}{\left(k^{\max}-k(L,t+\theta)+B(L,t+\theta)\left(L-\hat{x}+\frac{\theta-u_0\hat{x}}{w_0}\right)\right)^2},$$

is negative if $B(L,t+\theta)$ is in some interval $[-\underline{B}_{\text{high}}, \bar{B}_{\text{high}}]$ around zero. If we multiply the first term u_0+w_0 by the denominator, we obtain a quadratic equation in terms of $B(L,t+\theta)$, with positive and negative roots. Similarly, in the case of a quadratic fundamental diagram, the travel time (16) is decreasing with the shock location $\hat{x}$ for some range of values of $B(L,t+\theta)$ around zero.

As a result, a flow increase in period $s \leqslant t$, with $s+\tau(L,s) \leqslant t+\theta$, will decrease the shock location, and hence increase the travel time of a vehicle departing at time t.

Thus, the proposed travel-time functions only depend on past flows. Moreover, their derivative with respect to the current flow is positive in the case of a quadratic fundamental diagram, and nonnegative in the case of a triangular fundamental diagram. As a result, the Jacobian matrix is positive (semi-)definite. □

Incidentally, the Jacobian matrix is lower triangular, consistent with the principle of causality (Daganzo 1995b) that states that the travel time can only be affected by current or previous flows.

4.3. First-In-First-Out (FIFO)

The first-in-first-out (FIFO) condition guarantees that a vehicle that departed later cannot arrive earlier. The FIFO property gives consistency to the model, especially when one computes the path travel times as the sum of the link travel times. However, despite its nice analytical and computational properties, FIFO is not always verified in practice (e.g., in multilane intersections).

In the next theorem, we prove that the travel-time functions (12) and (16) satisfy the FIFO property for the particular case where $\theta=\tau(t-1)-1$ and $B(L,t+\theta)=0$.

THEOREM 5. *If* $\theta=\tau(t-1)-1$ *and* $B(L,t+\theta)=0$, *there exists a range of values for* $B(0,t)$ *around zero such that the travel-time functions* (12) *and* (16) *satisfy the FIFO property.*

PROOF. Satisfying FIFO means that the derivative of the travel time with respect to time, i.e., $d\tau/dt$ is greater than or equal to -1. For the triangular fundamental diagram, the free-flow travel time does not depend on previous flows, and the travel-time function is defined by (18). Because $f(0,t)/f(L,t+\theta)>0$, the difference between $\tau(L,t)$ and $\tau(L,t-1)$ is greater than -1. The travel-time function in the case of a quadratic fundamental diagram (16) is a polynomial of $B(0,t)$, and so is $d\tau/dk$. Because FIFO is satisfied when $B(0,t)=0$ as (16) simplifies to (18), there is a range of values around zero for $B(0,t)$ for which the property is also satisfied. □

The FIFO property can be shown in more general cases, but we omit the proof for the sake of brevity.

5. Integration Within a DUE Problem

5.1. Path Formulation of the DUE

The model for traffic delays can be embedded within a DUE setting. In this subsection, we propose a standard path formulation of a discrete-time DUE, defined on a time-expanded transportation network (see Ran and Boyce 1994).

Let us consider a network with a set of arcs A and a set of paths P, over a time horizon of T periods. Let W be the set of all origin-destination (OD) pairs. For a particular OD pair $w \in W$, let $P^w \subset P$ be the set of paths linking this origin to this destination, and let $d^w(t)$ be the given demand for period t. A DUE based on Wardrop's first principle satisfies the following property: If the flow on path $p \in P^w$ at time t, $f_p(t)$, is positive, the associated travel time $\tau_p(t)$ is minimal. Let $\pi^w(t)$ be the smallest travel time for the OD pair w at time t. Mathematically, Wardrop's first principle can be formulated as follows:

$$\tau_p(t)\begin{cases} = \pi^w(t) & \text{if } f_p(t)>0 \\ \geqslant \pi^w(t) & \text{if } f_p(t)=0 \end{cases} \quad \forall p \in P^w, \forall w \in W. \tag{19}$$

Stated differently, according to Wardrop's first principle, each traveler noncooperatively seeks to minimize his/her travel time. If path p consists of the m arcs $\{a_1, a_2, \ldots, a_m\}$, the path travel time for a vehicle starting its trip at time t, $\tau_p(t)$, is defined recursively as

$$\tau_p(t) = \tau_{a_1}(t) + \tau_{a_2}(t+\tau_{a_1}(t)) + \cdots + \tau_{a_m}\left(t+\tau_{a_1}(t)+\tau_{a_2}(t+\tau_{a_1}(t))+\cdots\right), \tag{20}$$

where τ_{a_i}, $i=1,\ldots,m$, are the arc travel-time functions defined in (12) or (16), depending on the assumed curve in the fundamental diagram.

In the following, we denote by $\mathbf{f}$ the vector of path flows for all periods, i.e.,

$$\mathbf{f} = \left(f_1(1), f_2(1), \ldots, f_{|P|}(1), f_1(2), \ldots, f_1(T), \ldots, f_{|P|}(T)\right),$$

associated with a vector of path travel times $\boldsymbol{\tau}(\mathbf{f})$. A vector of path flows is feasible if it is nonnegative and if it satisfies the demand, that is, if it belongs to the following polyhedron:

$$\mathcal{K} = \left\{\mathbf{f}:\ \sum_{p\in P^w} f_p(t) = d^w(t)\ \forall w \in W, \mathbf{f} \geqslant \mathbf{0}\right\}.$$

Wardrop's first principle can be expressed as the following variational inequality (see Nagurney 1993):

$$\boldsymbol{\tau}^*(\mathbf{f})'[\mathbf{f}-\mathbf{f}^*] \geqslant 0 \quad \forall \mathbf{f} \in \mathcal{H}. \tag{21}$$

However, there is no guarantee for the existence and the uniqueness of a solution to this variational inequality in a discrete-time setting. Even if the arc travel-time function (12) is continuous (see Theorem 3), the path travel times can be discontinuous because (20) involves discrete-time indices. This problem would not occur with a continuous-time formulation; however, the variational inequality would have infinite dimension.

On the other hand, even if the Jacobian matrix of the arc travel times (16) is positive definite (see Theorem 4), the Jacobian matrix of the path travel times is much more complex to analyze because it relies on the path flow pattern (if a path flow increases, it may affect the travel time of another path flow that shares some arcs in common) and the network structure (the capacity at the exit of an arc, $Q(t)$, depends on the flow exiting adjacent arcs). In particular, the Jacobian matrix of the path travel times is not necessarily lower triangular because the travel time of a flow starting its trip at time t might be affected by a flow on another path departing some time later. Further research is needed to characterize the structure of the Jacobian matrix of the path travel times. Alternatively, one could consider a formulation of the variational inequality in terms of arcs.

5.2. Path Flow Disaggregation

Formulating (21) relies on mapping path flows into path travel times. However, in §3 we only mapped arc flows into link travel times. To use our previous results, we need to develop a procedure for disaggregating path flows into link flows. Once we know the link flows, we can easily compute the link travel times with (12) or (16) and obtain the path travel times through (20).

We first outline the general procedure for the path flow propagation. Working with one path at a time, we start propagating the path flow from the path origin and continue propagating it along the path, moving forward in time. Specifically, if the path consists of arcs $a_1, a_2, \ldots$, we first compute the travel time on a_1 of the path flow starting its trip at time t, $\tau_{a_1}(L_{a_1}, t)$. Then, we propagate the path flow along a_1, and we compute its travel time on a_2 given that it is at the entrance of a_2 at time $t+\tau_{a_1}(L_{a_1}, t)$, and so on.

However, to compute the link travel time, one needs the total incoming flow, and not only the flow related to that particular path. Therefore, we stop propagating the path flow as soon as we encounter a link on the path at which not all path flows have arrived. If some path flows are waiting at link l for other path flows before being propagated, we say that link l is "blocking." As a result, the path flow is propagated along the path until it reaches either its destination or a blocking link.

In our implementation, we have initialized to -1 all cumulative arrivals and departures on link l associated with path p, denoted by $A_l^p(t)$ and $D_l^p(t)$, respectively, for all links l, all paths p that use link l, and all time periods t. Therefore, the flow can be propagated on link l if all but one path flow have arrived. A procedure for counting the number of path flows that have not arrived to link l at time t is outlined in Procedure 1.

Once the path flow has been propagated along link l at time t, all links downstream of l are examined, one at a time up to period $t+\tau_l(L_l, t)$, and the flow is propagated along these links if the links are not blocking. In Procedure 2, we maintain a list of active links, U, from which we branch out in the network. Once the flow is propagated on some link l, we add to the list of active links all links downstream of l. Note that we add several copies of each of them because the flow that has arrived on link l at time t exits the link some time between the last departure time, $t-1+\lceil\tau_l(L_l, t-1)\rceil$, and the next one, $t+\lfloor\tau_l(L_l, t)\rfloor$.

The procedure described above is repeated for each departure time of each path. We define a list of active paths, Q, and an order on the paths to propagate the flow as far as possible into the network. For each path p, we denote by t_p the maximum exit time of some path flow on a link in the network. This measures the progression of the flow into the network. A path flow that is blocked in the upstream links of the network will be associated with a small t_p, and conversely, a path flow that encounters no blocking link will have a large t_p. In Procedure 2, this quantity is updated in the link flow propagation module. Therefore, to avoid blocking links, we choose to process the paths in increasing order of t_p. Note that this order changes dynamically. Once a path has been examined T times, no flow will enter the network, and the path is deleted from the set Q.

In Procedure 2, we compute the link travel time for several path flows. So far, we have analyzed the travel time of vehicles with the same destination. In particular, the travel-time function that we derived depends on the ratio of the incoming flow over the exit capacity (see (18)). When there

Procedure 1. Number of path flows that have not arrived to link (l, t).

```
Count = 0
for all p ∈ P: l ∈ p do
  if path p does not start with l then
    u = link preceding l on path p
    if D_u^p(t) = −1 then
      Count = Count + 1
    end if
  else
    if A_l^p(t) = −1 then
      Count = Count + 1
    end if
  end if
end for
return Count
```

Procedure 2. Path flow propagation.

$Q = P$ (list of active paths)
for all $p \in P$ **do**
  $A_l^p(t) = D_l^p(t) = -1 \ \forall l, t$
  $t_p = 0$
end for
while $Q \neq \varnothing$ **do**
  $p = \arg\min_{p \in Q}\{t_p\}$
  $l =$ first link on path p
  List $U \leftarrow l$ (list of active links)
  while $U \neq \varnothing$ **do**
    $l =$ first link in list U
    $U \leftarrow U \setminus l$
    $t =$ smallest time period for which $A_l^p(t) = -1$ for some $p \in P$
    if (path p starts with l) and ($t = T$) **then**
      $Q \leftarrow Q \setminus p$
    end if
    if Number of path flows that have not arrived to link $(l,t) = 1$ **then**
      Travel time computation (l,t)
      Link flow propagation (l,t)
      for all $s = \lceil \tau_l(L_l, t-1) - 1 \rceil$ to $\lfloor \tau_l(L_l, t) \rfloor$ **do**
        for all $d \in D(l)$ **do**
          $U \leftarrow U \cup d$ (Branching out)
        end for
      end for
    end if
  end while
end while

Procedure 3. Travel-time computation (l,t).

$\theta = \lfloor \tau(L_l, t-1) - 1 \rfloor$
for all $d \in D(l)$ **do**
  $CAP_d = \min\{Q_d, D_d(L_d, t+\theta+1) - A_d(0, t+\theta) + k_d(L_d, t+\theta)L_d\}$
  $CAP_d = CAP_d - \sum_{u \in U(d), u \neq l} f_{u,d}(L, t+\theta)$ (remove flows outgoing from other links)
  $F_d = 0$
  for all $p \in P$: $l, d \in P$ **do**
    if p starts with l **then**
      $F_d = F_d + f_p(t)$ (add flow at the path origin)
      $A_l^p(t) = A_l^p(t-1) + f_p(t)$
    else
      $u =$ link preceding l on path p
      $F_d = F_d + D_u^p(t) - D_u^p(t-1)$ (add flow coming from upstream links)
      $A_l^p(t) = D_u^p(t)$
    end if
  end for
  $\tau_d = \tau_l(L_l, t-1) - 1 + F_d / CAP_d$ (travel time associated with downstream link d)
end for
$\tau_l(L_l, t) = \max\{L_l u_{0,l}, \max_{d \in D(l)}\{\tau_d\}\}$

are several downstream links, it is not clear how to compute the exit capacity, as it depends on the different priorities (e.g., special lane for right turns). In our simulation, we assumed that there was only a single lane on each arc and no priorities. Accordingly, in our setting, if a flow associated with a particular path is jammed, all flows associated with the other paths are also jammed.

Consider all path flows on link l, whose next link is the downstream link d. If there were only these path flows on link l, the travel time would be a function of the ratio of the sum of these path flows over the capacity of link d. If link d is the tightest bottleneck at the exit of link l, all other path flows will have the same travel time. Therefore, having clustered the path flows by downstream link, the travel time on link l is the maximum of the travel times of all clusters. Kuwahara and Akamatsu (2001) proposed a similar procedure by allocating the capacity of a downstream link d in proportion of the incoming flows whose next link is link d.

In a diverging intersection (one-to-many), the capacity of a downstream link d in period $t+\theta$ is computed as the minimum between the static link capacity Q_d and the dynamic link capacity, if there is queue spillback, $D_d(L_d, t+\theta+1) - A_d(0, t+\theta) + k_d(L_d, t+\theta)L_d$. In a more general intersection, link d can have several upstream links other than link l. Therefore, the downstream link capacity needs to be reduced to take into account the flow coming from these other upstream links. If these incoming flows are not known in time t (because these path flows have not arrived yet to link d, being blocked upstream), we estimate these flows from the past flows, taking a linear interpolation.

In the case of a triangular fundamental diagram and with $\theta = \tau_l(L_l, t-1) - 1$, the dynamic effects at the entrance $B(0,t)$ have no influence, and the dynamic effects at the road exit $B(L,t)$ are negligible. Therefore, the travel-time function can be fairly accurately approximated as the maximum between the free-flow travel time and the travel time with shock (18). In fact, if the downstream link d has a bottleneck capacity CAP_d and a flow F_d is incoming to link l with destination d, one can show that there is a shock if and only if $CAP_d(\theta - L_l u_{0,l}) < F_d$, i.e., if $L_l u_{0,l} < \theta + F_d / CAP_d$.

Procedure 3 outlines the computation of the travel time on link l at time t. We denote by $D(l)$ and $U(l)$ the set of links downstream of l and upstream of l, respectively.

Once link travel time has been computed, the flow can be propagated along the link, following the general idea that $A(0,t) = D(L, t+\tau(L,t))$ detailed in Procedure 4. In addition, Procedure 4 measures the progression of each path flow into the network, t_p.

Procedure 4. Link flow propagation (l,t).

for all $p \in P$: $l \in p$ **do**
  for all $s = \lceil \tau_l(L_l, t-1) - 1 \rceil$ to $\lfloor \tau_l(L_l, t) \rfloor$ **do**

$$\lambda = \frac{(t+s) - (t - 1 + \tau_l(L_l, t-1))}{(t + \tau_l(L_l, t)) - (t - 1 + \tau_l(L_l, t-1))}$$

    $D_l^p(L_l, t+s) = \lambda A_l^p(0,t) + (1-\lambda) A_l^p(0, t-1)$
  end for
  $t_p = \max\{t_p, t + \lfloor \tau_l(L_l, t) \rfloor\}$
end for

Figure 10. A two-link network example.

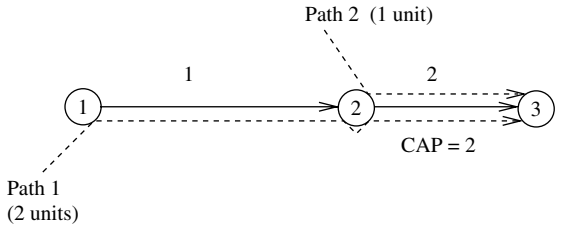

EXAMPLE. To illustrate the procedure we just described, let us consider the two-link network displayed in Figure 10. We denote by link 1 the upstream arc and by link 2 the downstream arc. Link 1 has infinite capacity, while link 2 has a capacity of 2. The free-flow travel times are equal to 1 for both links. We consider two paths, during two periods of time. Path 1 goes along link 1 and link 2 and has zero units of flow in the first period, and two units of flow in the second period. Path 2 goes along link 2 only, and has zero units of flow in the first period and one unit of flow in the second period.

We initialize $Q=\{1,2\}$. In the first iteration, the two measures of progression of the paths, t_1 and t_2, are set to zero. We arbitrarily select path 1 to start with. In period 1, path 1 has zero units of flow that will travel at the free-flow speed; therefore, $A_1^1(1)=0=D_1^1(s)$ for $s\leqslant 2$, and t_1 is updated to 2. The flow cannot be propagated on link 2 because the flow from path 2 has not arrived yet. We say that link 2 is blocking.

Because $0=t_2<t_1=2$, we select path 2 in the second iteration. Path 2 has zero units of flow in the first period, $A_2^2(1)=0$. The flow on link 2 in period 1 is the sum of flows of paths 1 and 2, i.e., $F=f_2(1)+(D_1^1(1)-D_1^1(0))=0$. This zero flow will travel at the free-flow speed. Therefore, $D_2^p(s)=0$ for $p=1,2$ and $s\leqslant 2$; t_2 is updated to 2.

Because $t_2=t_1=2$, we arbitrarily pick path 2 in the third iteration. The flow on link 2 in period 2 is the sum of flows of paths 1 and 2, i.e., $F=f_2(2)+(D_1^1(2)-D_1^1(1))=1+0=1$ and will travel at the free-flow speed. Therefore, $D_2^1(3)=0$ and $D_2^2(3)=1$. As path 2 has been examined twice, it is deleted from Q.

The set of active paths Q contains only one element, path 1. The incoming flow is 2, and $A_1^1(2)=2$. The downstream capacity is equal to 2, from which we subtract the flow that came from path 2 in period $t-1+\tau_1(L_1,t-1)=2$, equal to 1. As a result, only one unit of capacity is available for the flow of path 1. The travel time is the maximum between the free-flow travel time, 1, and the travel time with shock, $\tau_1(L_1,1)-1+2/1=2$. Therefore, $D_1^1(4)=2$ and $D_1^1(3)=1$. The list of active links contains two copies of link 2, corresponding to the propagation of flow in periods 3 and 4.

Because no flow comes from path 2 in period 3, the flow from link 1 can be propagated downstream. As a result, $A_2^1(3)=1$. Because the flow propagates at the free-flow speed on the second link, $D_2^1(4)=1$.

Figure 11. An example network.

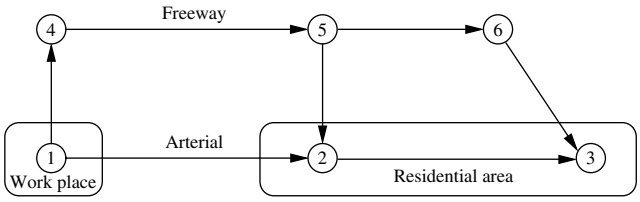

Likewise, because no flow comes from path 2 in period 4, the flow from link 1 can be propagated downstream. As a result, $A_2^1(4)=2$. Because the flow propagates at the free-flow speed on the second link, $D_2^1(5)=2$.

5.3. Numerical Example

To validate the procedure we introduced for solving DUE problems, we consider the transportation network test example with time-varying demands proposed by Kuwahara and Akamatsu (2001). As shown in Figure 11, this transportation network of six nodes and seven links is a simple model of a freeway and an arterial running parallel. The link data associated with a triangular fundamental diagram are shown in Table 1. We consider the evening commute, where users are going back from their work place to the residential area by taking either the freeway or the arterial. In particular, we consider two origin-destination pairs, $\{1,2\}$ and $\{1,3\}$, with the following traffic demand:

$$d^{\{1,2\}}(t)=\begin{cases}1{,}000 \text{ veh/hour},\\ \quad 0\leqslant t\leqslant 1 \text{ (h) and } 3<t\leqslant 5 \text{ (h)},\\ 2{,}000 \text{ veh/hour}, \quad 1<t\leqslant 3 \text{ (h)},\end{cases}$$

$$d^{\{1,3\}}(t)=\begin{cases}2{,}000 \text{ veh/hour},\\ \quad 0\leqslant t\leqslant 1 \text{ (h) and } 3<t\leqslant 5 \text{ (h)},\\ 4{,}000 \text{ veh/hour}, \quad 1<t\leqslant 3 \text{ (h)}.\end{cases}$$

In free flow, the freeway is the most attractive path to go from the work place to the residential area. For instance, for the OD pair $\{1,3\}$, the freeway free-flow travel time is 0.4 h, while the arterial free-flow travel time is 0.7 h. On the other hand, in the peak-traffic period, link $(6,3)$ will be saturated because it has a capacity of 3,000 vehicles/hour, while the peak demand is 4,000 vehicles/hour. As a result, a queue will appear and propagate backwards, and

Table 1. Link characteristics.

Link	u_0 (h/km)	w_0 (h/km)	$k^{\max}$ (veh/km)	Length (km)	$f^{\max}$ (veh/hour)
(1,4)	0.025	0.05	450	2	6,000
(4,5)	0.0125	0.05	375	16	6,000
(5,6)	0.0125	0.05	250	8	4,000
(6,3)	0.025	0.05	225	2	3,000
(1,2)	0.025	0.05	450	16	6,000
(2,3)	0.025	0.05	450	12	6,000
(5,2)	0.025	0.05	450	2	6,000

Algorithm 1. A dynamic Frank-Wolfe algorithm for solving (21).

Choose $\epsilon > 0$
$m = 0$,
$\mathbf{f}_p^m = \mathbf{0}\ \forall p \in P$
$\boldsymbol{\tau}^m = \boldsymbol{\tau}(\mathbf{f}^m)$ (free-flow travel times)
for all $w \in W$ **do**
  $p =$ shortest path w.r.t. $\boldsymbol{\tau}^m$
  $f_p^m(t) = d^w(t)\ \forall t = 1, \ldots, T$
end for
repeat
  $m \leftarrow m + 1$
  $\boldsymbol{\tau}^m = \boldsymbol{\tau}(\mathbf{f}^m)$ (see §5.2)
  $\mathbf{f}^* = \arg\max_{\mathbf{f}} \{(\boldsymbol{\tau}^m)'\mathbf{f}\colon \sum_{p \in P^w} f_p^w(t) = d^w(t)\ \forall w \in W, \mathbf{f} \geqslant 0\}$
    (linear optimization)
  if $\boldsymbol{\tau}(\mathbf{f}^*)'(\mathbf{f}^m - \mathbf{f}^*) < 0$ **then**
    Use binary search to find $\mathbf{f}^{m+1} = \lambda \mathbf{f}^m + (1-\lambda)\mathbf{f}^*$,
      $0 \leqslant \lambda \leqslant 1$, such that $\boldsymbol{\tau}(\mathbf{f}^{m+1})'(\mathbf{f}^m - \mathbf{f}^*) = 0$
  end if
until $\boldsymbol{\tau}(\mathbf{f}^m)'(\mathbf{f}^m - \mathbf{f}^*) < \epsilon$

the freeway will become less and less attractive in comparison to the arterial. As shown in Kuwahara and Akamatsu (2001), the impact of the queue spillback is so significant that a point queue model would not be appropriate for this example.

In our simulations, we considered five hours of traffic demand, discretized in time steps of 0.01 h, that is, we considered 500 time periods.

To solve the dynamic user equilibrium problem on this network, we implemented in C++ a dynamic version of the Frank-Wolfe algorithm. At every iteration, we solved a linear optimization problem, calling the CPLEX library, to solve the path formulation of the DUE, described in §5.1. The Frank-Wolfe algorithm for solving static variational inequality problems is fairly standard in the literature (e.g., see Martos 1975), and we outline it only briefly in Algorithm 1.

As shown in Figure 12, the algorithm made significant progress in the first iterations (in terms of the decrease of $\boldsymbol{\tau}(\mathbf{f}^m)'(\mathbf{f}^m - \mathbf{f}^*)$), but had trouble converging to zero thereafter. In fact, as we mentioned above, the path travel times are not necessarily monotone, and the algorithm is not a priori guaranteed to converge. However, from Figure 12, it seems that the algorithm would ultimately converge, but not monotonically.

The key issue in implementing this algorithm is the evaluation of the path travel times, which relies on the procedure described in §5.2. Even if the procedure for disaggregating path flows into link flows may seem cumbersome, it runs quickly. In fact, the first 30 iterations took less than a minute.

Figures 13 and 14 display the curves of the cumulative number of vehicles at the entrance of each link for the OD pairs $\{1,3\}$ and $\{1,2\}$, respectively. Because the path choice decisions are based on the actual travel time, and not the instantaneous travel time as in Kuwahara and Akamatsu

Figure 12. Convergence plot of the Frank-Wolfe algorithm.

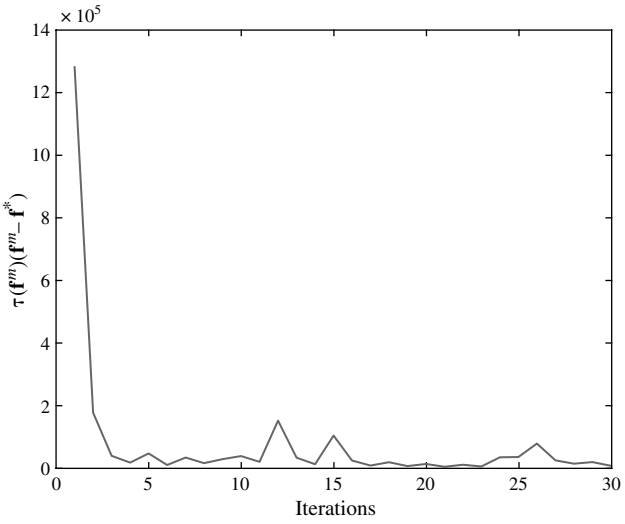

(2001), the figures are very different from Figures 6 and 7 in their paper.

For the OD pair $\{1,3\}$, the freeway is the first used path. As in Kuwahara and Akamatsu (2001), a queue completely covers link $(6,3)$ after 1.35 hours and spills back onto the previous link. After 1.75 hours, the queue also covers link $(5,6)$ and spills back onto link $(4,5)$. Note that because the capacity of link $(6,3)$ is fixed and there is no incoming flow into the freeway at the intermediate nodes, the density of the queue remains constant, and so is the travel time when the queue covers an entire link.

One significant difference with their model is that path $\{(1,2),(2,3)\}$ starts being used after 1.9 hours, and not after 2.09 hours. In fact, our model is based on the actual travel time and not the instantaneous travel time, and drivers anticipate the possible delays on the freeway earlier. Another difference with their results is that the two paths are never used simultaneously, while in Figure 13,

Figure 13. Cumulative link arrivals for the OD pair $\{1,3\}$.

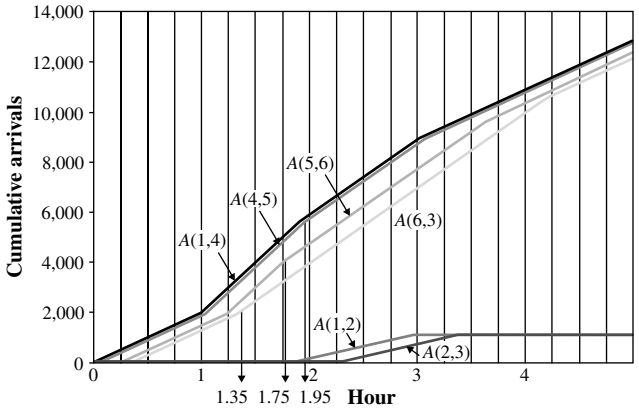

Figure 14. Cumulative link arrivals for the OD pair $\{1,2\}$.

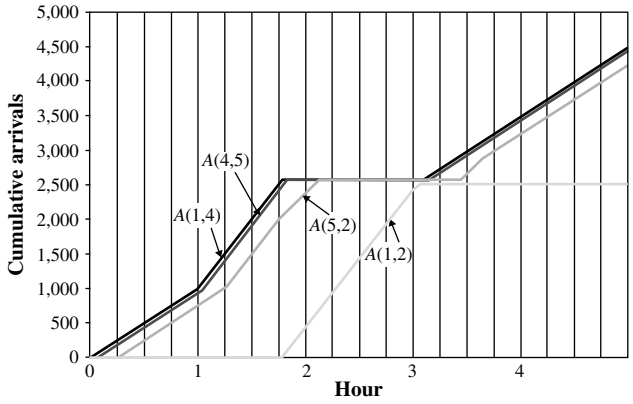

the curves of cumulative arrivals into $(1,4)$ and $(1,2)$ keep growing together. Specifically, in their model there is no flow incoming to link $(1,4)$ in the time intervals $[2.09, 2.29]$ and $[2.85, 3.15]$, as everything goes through the second path. The sudden switch of used paths that they observed seems to be a consequence of the path choice based on the instantaneous travel times. In their model, even though everybody decides to take an alternate path, the instantaneous travel time of the original path keeps increasing, deterring future flow to choose this path.

For the OD pair $\{1,2\}$ (see Figure 14), the effects of the queue originating from link $(6,3)$ have an impact on the travel time of link $(4,5)$ in period 1.75, as the queue backs up into link $(4,5)$. Because the travel time is increasing, the arterial is becoming more and more attractive. In period 1.79, the arterial is so attractive that all flow is taking it. In contrast, in Kuwahara and Akamatsu's (2001) model, the drivers did not anticipate the queue on the freeway, and the switch to the arterial only occurs after two hours. Moreover, in our model, the arterial is being used during the whole peak period, as the queue on the freeway does not decrease. With the instantaneous travel-time decisions, because there are two switches from the freeway to the arterial, and then from the arterial to the freeway for the OD pair $\{1,3\}$ during the peak period, the travel time on the freeway decreases after 2.34 hours, making the arterial less attractive.

In addition, we can observe that the principle of optimality is maintained dynamically. For example, if one of the shortest paths for OD $\{1,3\}$ in period 2 is $\{(1,2),(2,3)\}$, one of the shortest paths for OD $\{1,2\}$ in the same period is $\{(1,2)\}$. This observation may be used to speed up the solution of the DUE problem.

6. Conclusions

In this paper, we proposed a methodology for deriving an analytical travel-time function based on the theory of kinematic waves. In particular, we derived a travel-time function in the cases of triangular and quadratic fundamental diagrams. The derived travel-time function integrates first-order traffic dynamics as well as shock waves. Moreover, we illustrated numerically that this travel-time function is very consistent with the simulated travel times proposed in the literature.

With the advent of advanced transportation management systems (ATMS), a lot of attention has been devoted to solving the dynamic user equilibrium problem. We showed that the travel-time function that we derived can be incorporated within a DUE setting because it is (strictly) monotone and satisfies the FIFO property under certain conditions. As an illustration, we applied our model to a simple evening commute problem, emphasizing the dynamic nature of the traffic assignment.

Further research is necessary to develop a mathematical formulation of the flow propagation proposed in §5. A mathematical formulation of the problem, defined in terms of links instead of paths, would take advantage of the continuity and the (strict) monotonicity of the travel-time functions derived in §4. Moreover, the model needs to be enriched to capture local triggers of congestion such as deadlocks (on cyclic networks), traffic lights, multilane roads, etc. Finally, the proposed model for delays can be incorporated into more general or alternative traffic assignment problems such as the system equilibrium, the stochastic DUE, or the DUE with departure-time choices.

Appendix. Existence of at Most One Shock in the Case of a Quadratic Fundamental Diagram

Potentially, a shock could result from the focusing of two even forward waves or two even backward waves. We will impose a condition eliminating these cases. This will imply that there is at most one shock on every road, occurring when forward waves intersect backward waves.

Let us first consider two characteristic lines associated with forward waves, one emanating from the origin 0, and the other emanating from some arbitrary location y, with respective positive slopes defined according to Assumption A1. That is,

$$\frac{df(k(0,t))}{dk} = v^{\max}(1-2k(0,t)/k^{\max}) \quad \text{and}$$

$$\frac{df(k(y,t))}{dk} = v^{\max}(1-2(k(0,t)+B(0,t)y)/k^{\max}).$$

A shock occurs at the intersection of these two characteristic lines, at location $\hat{x} = (k^{\max} - 2k(0,t))/(2B(0,t))$. Because the shock location is independent of y, we conclude that all forward characteristic lines intersect each other at the same location.

Therefore, no local shock occurs if $\hat{x} > L$, that is, if $B(0,t) \leqslant (k^{\max}/2 - k(0,t))/L$. This is automatically satisfied if $0 \leqslant k(0,t) + B(0,t)L \leqslant k^{\max}/2$.

Similarly, for backwards moving waves, we consider two characteristic lines, one emanating from the destination L, and the other emanating from some location

$0 < y < L$. No local shock occurs if the shock location is below 0 (before the road entrance), i.e., $B(L,t) \leqslant (k(L,t) - k^{\max}/2)/L$. This is automatically satisfied if $k^{\max}/2 \leqslant k(L,t) - B(L,t)L \leqslant k^{\max}$.

Acknowledgments

The authors thank the associate editor and the anonymous referees for their insightful comments that significantly improved this paper. This work was partially supported by the PECASE award DMI-9984339 from the National Science Foundation and the Singapore-MIT Alliance Program.

References

Carey, M., Y. E. Ge, M. McCartney. 2003. A whole-link travel-time model with desirable properties. *Transportation Sci.* **37**(1) 83–96.

Cayford, R., W.-H. Lin, C. F. Daganzo. 1997. The NETCELL simulation package: Technical description. Research report UCB-ITS-PRR-97-23, University of California, Berkeley, CA. http://www.ce.berkeley.edu/~daganzo.

Daganzo, C. F. 1994. The cell transmission model: A dynamic representation of highway traffic consistent with the hydrodynamic theory. *Transportation Res. B* **28**(4) 269–287.

Daganzo, C. F. 1995a. The cell transmission model. Part II: Network traffic. *Transportation Res. B* **29**(2) 79–93.

Daganzo, C. F. 1995b. A finite difference approximation of the kinematic wave model of traffic flow. *Transportation Res. B* **29**(4) 261–276.

Daganzo, C. F. 1995c. Properties of link travel time function under dynamic loads. *Transportation Res. B* **29**(2) 95–98.

Edwards, C. H., Jr., D. E. Penney. 1985. *Elementary Differential Equations with Boundary Value Problems*, 3rd ed. Prentice Hall, Englewood Cliffs, NJ.

Friesz, T. L., D. Bernstein, T. E. Smith, R. L. Tobin, B.-W. Wie. 1993. A variational inequality formulation for the dynamic user equilibrium problem. *Oper. Res.* **41**(1) 179–191.

Gazis, D., R. Herman, R. W. Rothery. 1961. Nonlinear follow-the-leader models of traffic flow. *Oper. Res.* **9**(4) 545–567.

Greenshields, B. 1935. A study of traffic capacity. *Highway Res. Board Proc.* **14** 468–477.

Haberman, R. 1977. *Mathematical Models; Mechanical Vibrations, Population Dynamics and Traffic Flow.* Prentice-Hall, Englewood Cliffs, NJ.

Herman, R., E. W. Montroll, R. B. Potts, R. W. Rothery. 1959. Traffic dynamics: Analysis of stability in car following. *Oper. Res.* **7** 86–106.

Hurdle, V., B. Son. 2000. Road test of a free way model. *Transportation Res. B* **34**(7) 537–564.

Kachani, S., G. Perakis. 2001. Modeling travel times in dynamic transportation networks: A fluid dynamics approach. Working paper, Massachusetts Institute of Technology, Cambridge, MA.

Khoo, B. C., G. C. Lin, J. Peraire, G. Perakis. 2002. A dynamic user-equilibrium model with travel times computed from simulation. Working paper, Massachusetts Institute of Technology, Cambridge, MA.

Kuwahara, M., T. Akamatsu. 2001. Dynamic user optimal assignment with physical queues for a many-to-many OD pattern. *Transportation Res. B* **35** 461–479.

Li, J., O. Fujiwara, S. Kawakami. 2000. A reactive dynamic user equilibrium model in a network with queues. *Transportation Res. B* **34** 605–624.

Lighthill, M. J., G. B. Whitham. 1955. On kinematic waves: II. A theory of traffic flow on long crowded roads. *Proc. Roy. Soc. A* **229** 317–345.

Lin, W.-H., H. K. Lo. 2000. Are the objectives and solutions of dynamic user-equilibrium models always consistent? *Transportation Res. A* **34** 137–144.

Mahut, M. 2000. Discrete flow model for dynamic network loading. Ph.D. thesis, Département d'informatique et de recherche opérationnelle, Université de Montréal, Montréal, Quebec, Canada.

Martos, B. 1975. *Nonlinear Programming. Theory and Methods.* North-Holland, Amsterdam, The Netherlands.

Nagurney, A. 1993. Network economics: A variational inequality approach. *Advances in Computational Economics*, Vol. 10. Kluwer Academic Publishers, Boston, MA.

Newell, G. F. 1993. A simplified theory of kinematic waves in highway traffic, I. General theory; II. Queuing at freeway bottlenecks; III. Multidestination flows. *Transportation Res. B* **27**(4) 281–314.

Patriksson, M. 1994. The traffic assignment problem: Models and methods. *Topics in Transportation.* VSP BV, Zeist, The Netherlands.

Perakis, G. 2000. Dynamic traffic flow problems: A hydrodynamic theory approach. Working paper, Massachusetts Institute of Technology, Cambridge, MA.

Ran, B., D. E. Boyce. 1994. Dynamic urban transportation network models. *Lecture Notes in Economics and Mathematical Systems,* Vol. 417. Springer-Verlag, Berlin, Germany.

Ran, B., N. M. Rouphail, A. Tarko, D. E. Boyce. 1997. Toward a class of link travel time functions for dynamic assignment models on signalized networks. *Transportation Res. B* **31**(4) 277–290.

Richards, P. I. 1956. Shock waves on the highway. *Oper. Res.* **4** 42–51.

Schrank, D., T. Lomax. 2003. The 2003 annual urban mobility report. Technical report, Texas Transportation Institute. http://mobility.tamu.edu/ums/report/.

Velan, S. 2000. The cell transmission model: A new look at a dynamic network loading model. Ph.D. thesis, Centre de Recherche sur les Transports, Université de Montréal, Montréal, Quebec, Canada.

Ziliaskopoulos, A. K. 2000. A linear programming model for the single destination system optimum dynamic traffic assignment problem. *Transportation Sci.* **34**(1) 37–49.